

Comparative assessment of advanced power generation and carbon sequestration plants on offshore petroleum platforms

Fernanda Cristina Nascimento Silva^a, Ronaldo Lucas Alkmin Freire^b, Daniel Flórez-Orrego^c and Silvio de Oliveira Junior^d

^a *University of Sao Paulo, Sao Paulo, Brazil, fernanda.nascimento.silva@usp.br*

^b *University of Sao Paulo, Sao Paulo, Brazil, rlafreire@usp.br,*

^c *University of Sao Paulo, Sao Paulo, Brazil, dafloreso@usp.br,*

^d *University of Sao Paulo, Sao Paulo, Brazil, soj@usp.br.*

Abstract:

On conventional offshore petroleum platforms, the combined heat and power production (CHP) currently depends on simple cycle gas turbine systems (SCGT) that operate at lower efficiency and increased environmental impact, compared to modern onshore thermoelectric plants. Additionally, the reduced space and the limited weight budget on offshore platforms have discouraged operators from integrating more efficient, but also bulkier cogeneration cycles (e.g. combined cycles). In spite of these circumstances, more stringent environmental regulations of offshore oil and gas activities have progressively led to a renewed interest in the integration of advanced cogeneration systems, together with either customary or unconventional carbon capture approaches, to maintain both higher power generation efficiencies and reduced CO₂ emissions. Thus, in this paper, it is evidenced how advanced gas turbine concepts are promising technologies for maintaining or even increasing efficiency, while facilitating the capture rate of CO₂ produced, either for geological storage or enhanced oil recovery. Despite the profuse research works on onshore applications, advanced cogeneration and carbon capture systems have been barely studied in the context of supplying the power to offshore petroleum platforms. Accordingly, the performance of a conventional offshore petroleum production platform (without carbon capture system) is for the first time compared to other configurations, based on either an amines-based chemical absorption system or oxyfuel combustion concepts (e.g. S-Graz and Allam cycles) for CO₂ capture purposes. Since the original power and heat requirements of the processing platform must remain satisfied, an energy integration analysis is performed to determine the waste heat recovery opportunities. Additionally, the exergy method helps quantifying the most critical components that lead to the largest irreversibility and identifying the thermodynamic potential for enhanced cogeneration plants. As a result, oxyfuel equipped platforms provide a diversified set of advantages, while keeping competitive efficiencies. For instance, advanced systems allow for cutting down ostensibly the atmospheric CO₂ emissions compared to the conventional and amines-based power plant configurations of the FPSO.

Keywords:

Power generation; Petroleum production; Offshore platforms; Oxyfuel technology; Carbon capture.

1. Introduction

The dramatic escalation of the climate crisis has encouraged prompt efforts from all around the world in order to contain the disastrous effects of climate change to a minimum [1, 2]. Governments, private companies, academic and civil institutions have committed to research, fund and support initiatives and technology that promote carbon dioxide emissions reduction. The

attention is especially focused on the energy sector, responsible for over a third of those discharges [3]. Such concerns are justified considering that the production of utilities currently relies mostly on fossil fuels, and the practice of geological storage of the produced carbon dioxide is still an exception [2]. Although a fossil-free energy economy would be preferable, the phase-out of fossil fuels still poses many questions and debates over how the transition towards a decarbonized future should occur. This uncertainty arises in part due to the extensive existing and incoming infrastructure required, economic and political interests as well as the characteristics of the various techniques and energy sources at hand [4, 5]. In fact, the most likely scenario seems to point at a diversified energy mix in which the solutions are closely integrated and, at the same time, decentralized [6, 7].

According to some estimates of the International Energy Agency [8], more restrictive scenarios that include carbon capture and storage (CCS) as a mitigation tool show that this technique might account for only less than 10% of the total reduction of emissions in 2040, out of which one third would be allocated to the power and industrial sectors. Moreover, among the different reported CCS techniques, oxyfuel systems seem the most promising as they render the separation of the main combustion products (CO₂ and water) relatively easier, compared to conventional air-blown, post-combustion processes [5]. In the oxyfuel process, the fuel reacts with nearly pure oxygen (above 95% mol), resulting in a flue gas whose components can be easily separated via water condensation. Nonetheless, the energy savings in the flue gas purification stage are partially offset by the need for an additional air separation unit (ASU), which eventually impairs the overall efficiency of the system. Furthermore, in order to control the turbine inlet temperature and to avoid harmful material overheating, partial recycling of the flue gases produced is still required. Hot section temperatures could also be controlled by either injecting steam (alongside the gaseous fuel, the oxidizer and the recycled flue gas) into the combustor chamber or directly into the turbine. Such strategy is actually employed in various works [9, 10], as long as high temperature resistant gas turbines are not widely commercially available yet. More remarkably, by avoiding the emissions dilution in nitrogen, close to zero CO₂ emissions and lower NO_x power plants with higher efficiencies can be envisaged, while contemplating a wider variety of fuels [11].

Oxyfuel and chemical absorption carbon capture techniques are well-understood. However, the integration of such technologies in a Floating Production Storage and Offloading (FPSO) unit has barely or has not been studied at all, with most studies focusing on stand-alone assessments or on onshore applications. An offshore platform setting is a particularly challenging application scenario as it is energy intensive, with shifting lifetime energy demands as well as severe area, weight and stability restrictions. It is worthy to notice that some modern FPSOs already have membrane-based carbon separation and recompression systems, designed for geological storage of the CO₂ present in the petroleum basins targeted in this study, but the integration of advanced post-combustion CCS units is still under preliminary assessment [12, 13]. Accordingly, this work compares the overall performance of four FPSO configurations based on different cogeneration systems, intended to operate at the Brazilian Pre-salt gas reservoir conditions. The conventional case (i.e. FPSO sparing any CO₂ mitigation technology) is for the first time compared with another platform equipped with a simple cycle gas turbine, a waste heat recovery unit and a post-combustion CCS system. In addition, the integration of two oxyfuel cycles to the offshore platform, namely the S-Graz and the Allam cycles, is also analyzed. The exergy analysis and energy integration methods are used to propose suitable exergy efficiency definitions that allow for a fair level playing field when comparing the platform, cogeneration plant and component-wise performances of each configuration. An exergy destruction breakdown is also used to quantify and allocate the irreversibility among the main units composing the platform. Furthermore, an energy integration analysis is used to calculate the maximum potential heat recovery. Finally, the penalties associated to the introduction of an ASU and an amine-based carbon absorption unit are discussed. An auxiliary boiler may be also required to balance the waste heat deficit in the FPSO when integrating some advanced configurations. Finally, although the analysis of space and weight allowance in existing platforms is out of the scope of this paper, ongoing research works of the authors points

towards suitable alternatives to centralize the power demands of a cluster of FPSOs, so that the utility systems are not anymore constrained to the deck of the producing platform.

2. Layout of conventional, amine and oxyfuel-based platforms

Notably, the conventional platforms operating in Brazil are not equipped yet with carbon capture systems to mitigate the atmospheric emissions produced through the combined heat and power generation. Actually, this study is mainly motivated by recent commitments to the introduction of carbon capture systems in the existent and new Brazilian FPSOs [14], due to the increasing environmental regulations in the natural gas and oil industry. Accordingly, the advantages and challenges of the three proposed platform configurations with carbon capture systems, namely a chemical absorption-based setup using a typical aqueous amine solution (MEA, 30% wt.) and other two based on the so-called near to zero-emissions S-Graz and Allam (or NET Power) cycles, are thoroughly compared with the performance of a conventional configuration of an offshore petroleum platform.

Figures 1-4 depict the four types of plants studied in this paper, which are assumed to operate at the condition of highest oil production rate in an oilfield located at the Brazilian Pre-salt [15, 16]. It is also noteworthy that water production is not considered at this point of the lifetime of the well. The representative production rates of oil, CO₂ and natural gas are based on the reported literature [17-19] and briefly described in this section. For all the four configurations, petroleum is extracted from the well at a flow rate of 197 kg/s and goes through an energy intensive primary separation unit. The multiphase separation process of petroleum into natural gas, CO₂ and oil considers the specific energy consumption required to separate the mixture of around 160 kJ/kg [19-22]; or equivalently, a heat exergy demand close to 2 MW. After the primary separation, oil is pumped to the shore at a flow rate of 161 kg/s. Meanwhile, the separated gas phase is compressed to 52 bar [23] and sent through a membrane purification system, which separates it into a permeate methane-rich stream and a CO₂-rich stream that still contains a large amount of methane [24]. The stream composition after the membrane separation is such that the methane-rich stream (28 kg/s) is composed of approximately 97% of methane and 3% CO₂ (molar). Next, a fraction of the purified natural gas stream is fed as fuel into the cogeneration system (40 bar), or further compressed as in the case of the Allam cycle, which operates at much higher pressures (300 bar). The remaining methane-rich gas is compressed up to 245 bar to be exported to the shore. Meanwhile, the carbon dioxide-rich stream (approx. 8 kg/s), with a molar composition of 70% CO₂ and 30% methane, is compressed up to 450 bar, suitable for injecting it into the well for the sake of enhanced oil recovery (EOR).

The conventional configuration shown in Figure 1 is the most common one in the commercial scenario of the Brazilian FPSOs. In this design, high temperature gases (1150°C) are expanded in a simple cycle gas turbine (SCGT) to generate power, whereas the energy available at the turbine exhaust gases is used to raise hot water up to 150°C in a closed loop, which in turn will heat up the petroleum mixture in the primary separation system. The expanded cold flue gases (approx. 300 °C) at low pressure are eventually discharged to the atmosphere without any other procedure performed to capture the CO₂ content from the flue gas.

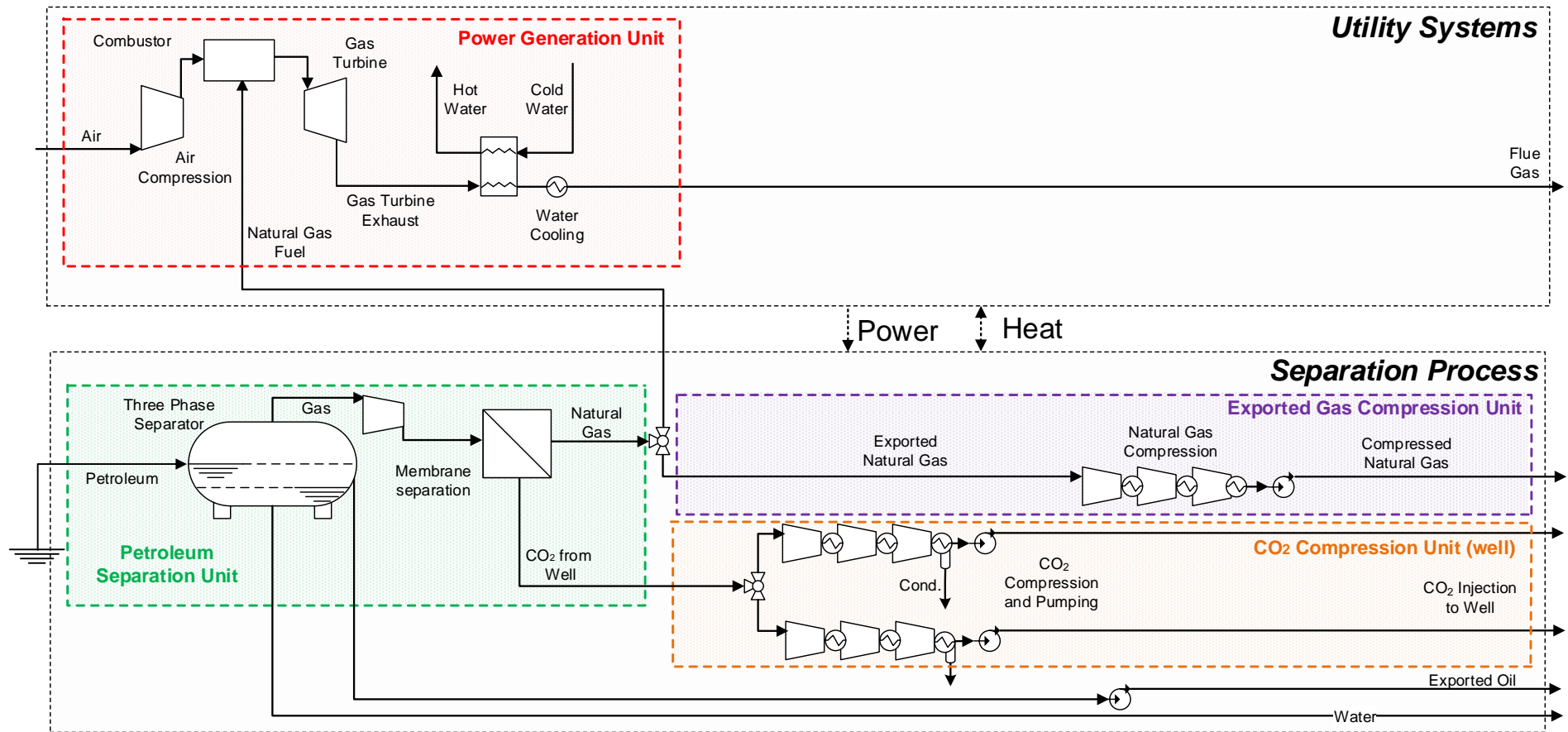


Figure 1. Conventional FPSO configuration powered by a simple cycle gas turbine system.

As concerns the amine-based configuration (Figure 2), the heat exergy in the gas turbine exhaust is not only used to supply the heat requirement in the primary separation unit, but also to raise the steam used as a means of providing the reboiler duty to desorb the captured CO₂ in the amine loop. In the latter process, monoethanolamine (MEA) is used to separate the CO₂ out of the combustion gases, before being compressed for re-injection purposes. The counterpart of this purified CO₂ stream is the purified flue gas discharged to the environment at close to atmospheric pressure. During the CO₂-rich stream compression stage, the remaining moisture content is continuously condensed (knockout) between compression steps. The dried CO₂ gas is further compressed to elevated pressures of about 450 bar, so it can be injected back into the well for EOR, thus partially mitigating the environmental impact.

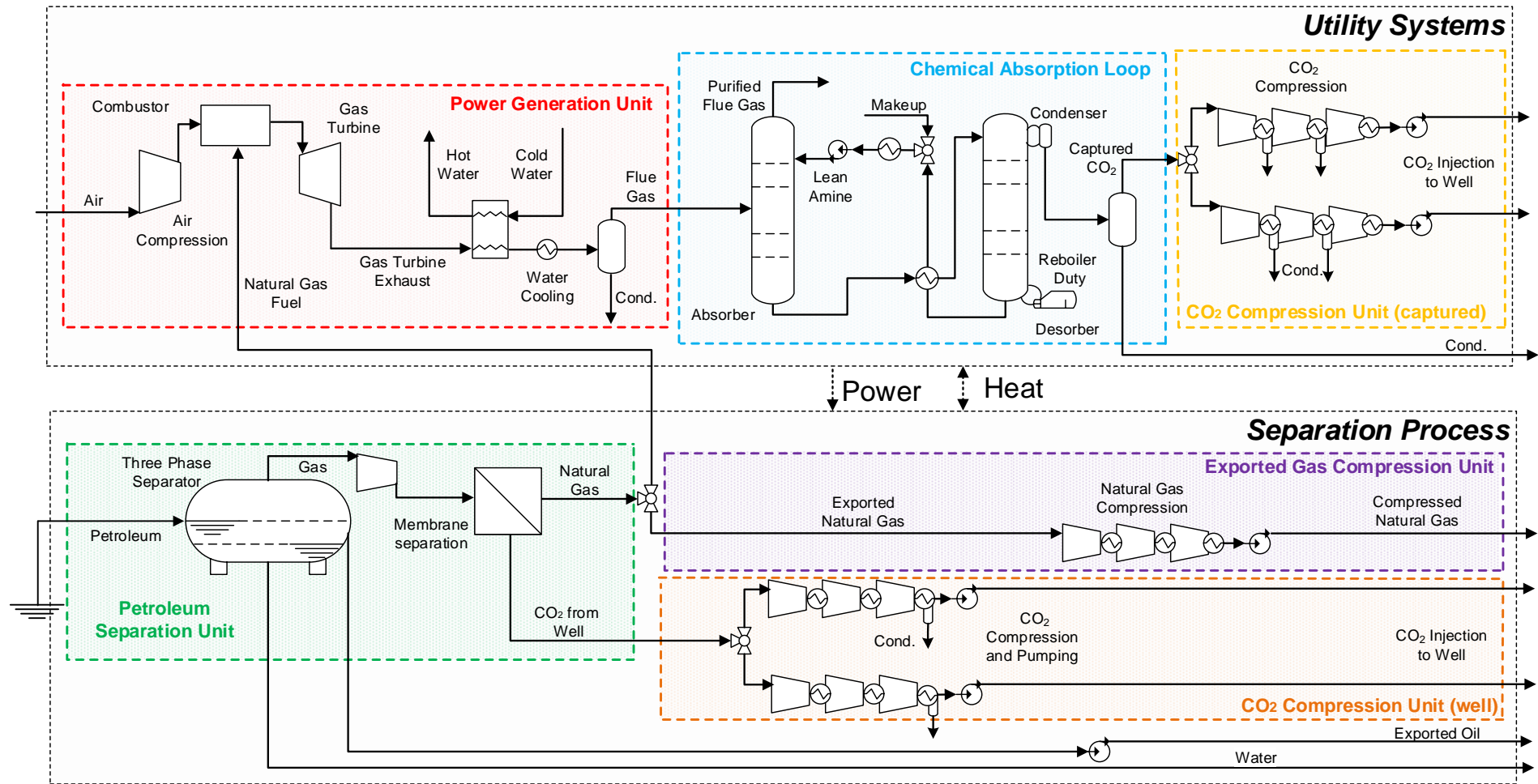


Figure 2. FPSO configuration based on a simple gas turbine cycle equipped with a chemical absorption carbon capture unit (monoethanolamine).

In this work, two oxyfuel power cycles are compared with the conventional FPSO layout and the one equipped with an amine-based post-combustion CCS unit. The first configuration considered is the S-Graz cycle as proposed by Wolfgang Sanz in 2005 and inspired by the original idea of the Graz cycle by Herbert Jericha in 1985 [9, 10, 25, 26]. This cycle was initially designed to run on hydrogen fuel and pure oxygen derived from water electrolysis [26], but delays in the development of hydrogen technology forced adjustments so that it could function with fossil fuels instead [27]. In the simplified flowsheet of the platform powered by an S-Graz cycle (see Figure 3), the primary separation unit of petroleum, the oil pumping, and the compression processes of the exported methane-rich gas and of the CO₂ rich-stream exiting the membrane separation process remain the same as in the previous configurations.

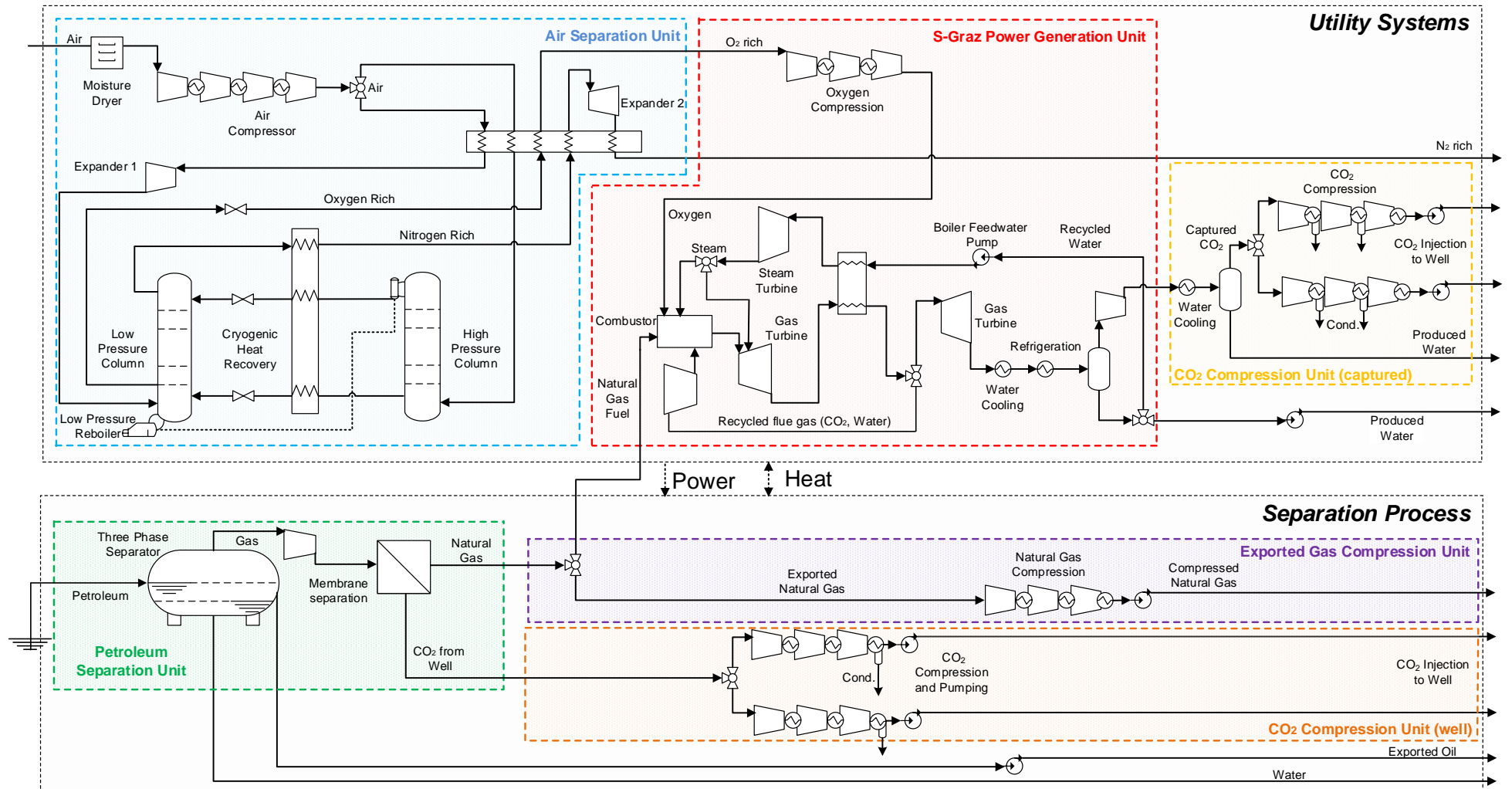


Figure 3. FPSO configuration powered by an S-Graz cycle.

However, as long as pure oxygen is used for combustion instead of normal air, an additional air separation unit (ASU) is required. Differently from the previous air-blown power generation units, in the S-Graz cycle, a fraction of the methane-rich gas is fired as fuel with an oxygen-rich stream at 40 bar. The recycled combustion gases (78% H₂O and 22% CO₂ molar) together with expanded steam are injected into the gas turbine combustor in order to control the oxyfuel gas turbine inlet temperature (1400°C). Furthermore, superheated steam (565 °C, 180 bar) is produced in a heat recovery steam generator by using the exhaust gases of the gas turbine, and expanded to produce more power before the steam injection [9]. It is important to point out that steam is not only injected to the combustor chamber, but also at the admission of the gas turbine. Furthermore, 71.5% of the total molar flow of the combustion gases produced is recirculated and compressed back to 40 bar before entering the combustor chamber. The remainder are further expanded (0.04 bar) and then cooled to 18°C by using a vapour compression refrigeration system, which partially separates the water in a vapour-liquid flash separator [9]. The captured CO₂ is then recompressed to pressures suitable for geological injection and storage, whereas the excess water produced in the combustion process is discarded to the sea.

The second oxyfuel cycle analyzed is the Allam or NET Power cycle, patented in 2011 [28, 29]. This oxyfuel cycle and the ensuing equipment have been developed through a partnership of multiple utility companies and manufactures [30]. As of November 2016, “a 50 MWth demonstration-scale natural gas version of the plant is currently in construction by NET Power to prove out the operability of the cycle and validate its performance, control methodology, operational targets, and component durability” [31]. A commercial scale 300MWe Allam Cycle plant is also underway and is expected to be finalized by the end of 2020. In May 2018, NET Power announced to have successfully achieved a “first fire of its supercritical carbon dioxide (CO₂) demonstration power plant and test facility located in La Porte, TX, including the firing of the 50 MWth commercial-scale combustor of Toshiba Energy Systems & Solutions Corporation ” [32]. In the Allam cycle, the involved pressures are much higher than in the previous three designed setups (see Figure 4). In this cycle, oxidant stream is formed by mixing a highly pure O₂ stream with a fraction of the recycled CO₂ flow, which enters the combustor chamber at 300 bar along with the pressurized methane fuel and some more recycled carbon dioxide. The flue gas resultant from the combustion flows towards the gas turbine inlet where it is joined by the remaining recycled flue gas to be expanded up to 30 bar.

After this expansion, the flue gas, mainly composed of CO₂, goes through a multiple-stream exchanger wherein heat is recovered by preheating the recycled and oxidant flows. Due to differences in heat capacity of carbon dioxide at radically different pressures and temperatures flowing through the waste heat exchanger, an additional amount of heat from an external source, in this particular case from the intercooling stages of the oxygen compression process, must be supplied to balance the heating requirements [31, 33]. In order to separate the moisture present in the combustion products, further cooling to 69°C must be performed. The whole of the highly pure CO₂ is initially compressed up to 100 bar, before 96.2% of the compressed stream is recycled back to the power generation unit, as shown in Figure 4, to compose the oxidant stream and recycled flows. The remainder is further compressed to re-injection pressures (the same as in previous configurations). Meanwhile, the air separation unit, the primary separation unit, the exported gas compression unit and injected CO₂-rich compression unit operate in a similar manner to all the other plant layouts. However, in the Allam cycle, a small amount of methane fuel must be burnt in an auxiliary boiler in order to meet the heating requirements of the FPSO that could not be satisfied by recovering waste heat elsewhere.

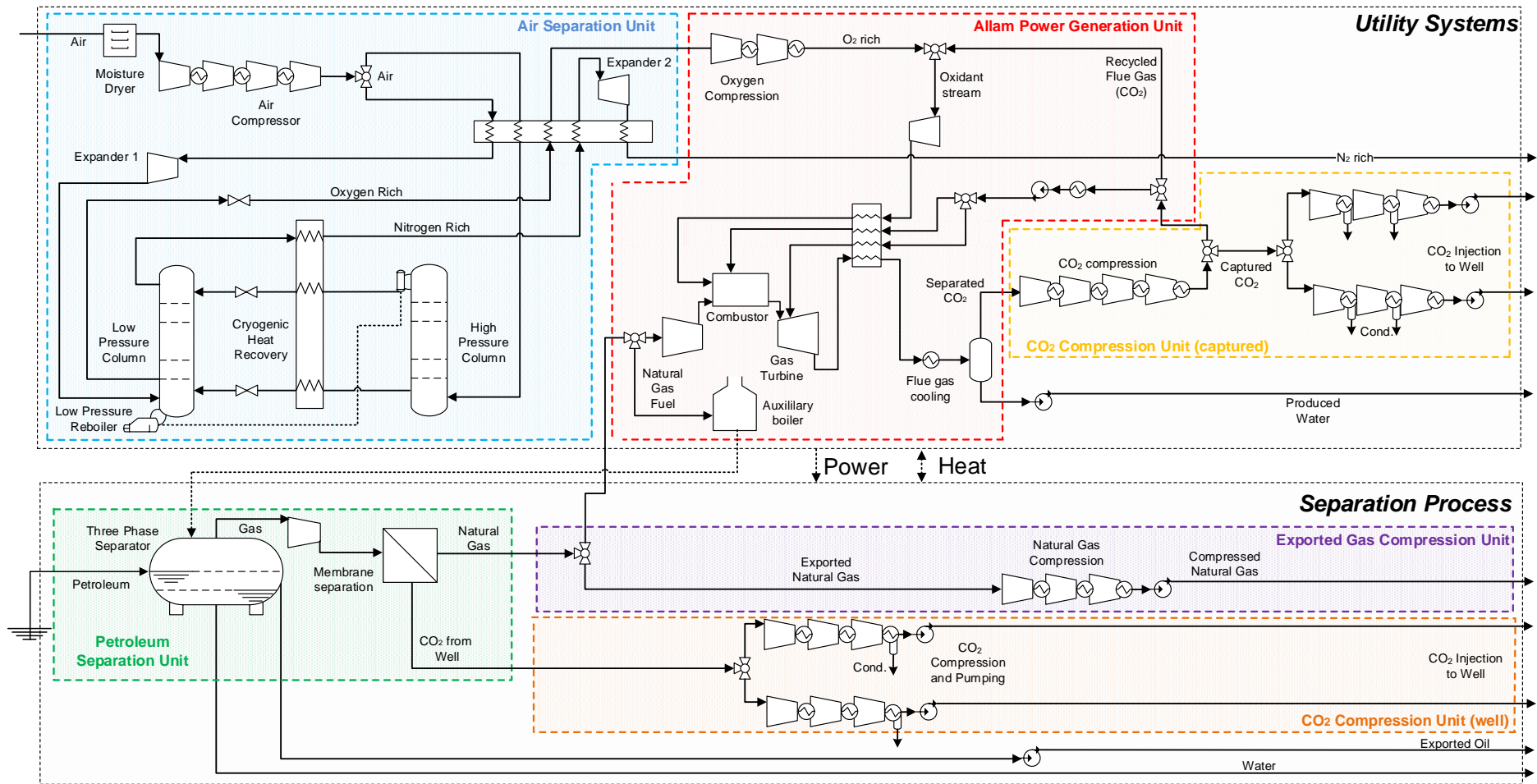


Figure 4. FPSO configuration powered by an Allam cycle.

2.1. Air separation unit

A cryogenic air separation unit (ASU) has been modeled to fulfil the oxygen requirement of the S-Graz and Allam power cycles. This technique was chosen since it is the most adequate when high gaseous oxygen flow rates are required at high purity [34]. In this unit, normal air at ambient conditions of 25°C and 1 bar is compressed up to 7.45 bar and 40°C. About 95% of the compressed air is cooled down in the main recovery heat exchanger (-170°C) and then it is fed into a high pressure separation column (HPC) [35]. The remaining 5% of the compressed air (-139°C) is expanded to 2.95 bar before entering the low pressure separation column (LPC). Next, both the liquid bottoms and vapour overhead outlet of the HPC are cooled down by using the nitrogen-rich stream coming from the LPC overhead, and then expanded and sent to the LPC wherein further air separation occurs. Both columns are thermally integrated as the HPC condenser provides the duty required by the LPC reboiler. A last expansion step (1 bar) of the nitrogen rich stream produced in the LPC allows for an increased cooling effect in the main heat exchanger [36]. The main ASU product corresponds to an oxygen-rich stream (99.5% molar). Clearly, this composition adds some advantages in terms of few inert gases in the combustion products, saving an extra step later on for inerts removal [37]. The other distillation product is a nitrogen-rich stream that could be either discharged to the environment or even commercialized.

3. Process modelling and performance indicators

In the following sections, a combined energy integration analysis and exergy assessment are used to determine the overall performance of the studied configurations, as well as of the utility systems thereof in terms of energy consumption, process irreversibility, and the thermodynamic potential for waste heat recovery. The methodology used for the allocation of the unit exergy costs and specific CO₂ emission among the representative streams of the studied platforms is also described, along with the proposed exergy efficiency definitions used to rank the performance of the advanced and conventional configurations.

Mass, energy and exergy balances of each sub-process of interest and the thermo-physical properties of each flow present in the system are carried out by using Aspen Hysys® V8.8 software. Physical and chemical exergy calculations, as well as exergy efficiencies are assessed through VBA® scripts as *user defined functions* [38]. Various performance indicators are proposed for each configuration so that objective comparisons between the different designed setups can be achieved. Table 1 displays three exergy efficiency definitions that allow different interpretations of the configurations studied. All equations are applied to control volumes that extend from air entering the air compression train to the release of flue gas as in the conventional case, or till the CO₂ captured to re-injection, as in the case of the S-Graz, Allam (incl. air separation, power generation and CO₂ compression units) and the amine-based CO₂ absorption cycle (power generation, MEA loop and CO₂ compression units). As it has been previously stated, the petroleum separation process remains invariable for all the control volumes.

Equation (1) aims to specifically evaluate the ability of the utility system to efficiently convert the chemical exergy of the fuel consumed into net power (i.e. already discounting the power demanded by the ASU, the power cycle ancillary equipment, such as pumps and recycling compressors, and the injection compression system). On the other hand, Equation (2) evaluates the capacity of the utility system to operate in a combined heat and power (CHP) generation mode by measuring how efficiently fuel chemical exergy is converted into the power and heat required by the gas and oil processing plant. Finally, Equation (3) measures the increase between the input and output total exergy as a result of the consumption of the fuel exergy. The last efficiency effectively contextualizes the main function of the FPSO unit, namely separating the petroleum into its products. It is important to stress that $\Delta\dot{B}_{total}$ is calculated with respect to the streams that are not consumed within the utility system; that is, the fuel stream consumed is discounted from the exergy input of natural gas. Moreover, the terms \dot{W}_{cycle} , \dot{W}_{pu} , \dot{B}_{WHRU}^Q and \dot{B}_{fuel}^{CH} refer to (i) the net power

produced, (ii) the power demand of the processing unit, (iii) the exergy associated to the waste heat recovery from flue gas at the turbine outlet and from the compression intercoolers also within the control volume, and (iv) the chemical exergy of the fuel stream, respectively.

Table 1. Overall exergy efficiencies proposed for the plantwide and component-wise FPSO unit.

Definition	Formula	Equation
Power	$\eta_{power} = \frac{\dot{B}_{useful, output}}{\dot{B}_{chemical, fuel}} = \frac{\dot{W}_{cycle}}{\dot{B}_{fuel}^{CH}}$	(1)
Cogeneration	$\eta_{cogen} = \frac{\dot{B}_{useful, output}}{\dot{B}_{chemical, fuel}} = \frac{\dot{W}_{pu} + \dot{B}_{WHRU}^Q}{\dot{B}_{fuel}^{CH}}$	(2)
Separation	$\eta_{sep} = \frac{\Delta \dot{B}_{total}}{\dot{B}_{consumed}} = \frac{\dot{B}_{total, output} - \dot{B}_{total, input}}{\dot{B}_{total, fuel}}$	(3)

Finally, it is worth noticing that previous works of Oliveira Jr. and van Hombeeck [39], Silva and Oliveira Jr. [18] and Carranza and Oliveira Jr. [15] have already used the exergy concept to calculate the performance of the offshore petroleum platforms in Brazil. Further studies [40-42] analyzed the processes present in the Brazilian petroleum refineries by using exergy as the efficiency indicator for the separation processes. Moreover, the exergy content has been suitably considered as a rational criterion for the allocation of the unit costs among the crude oil and the natural gas produced in offshore platforms that operate under the conventional configuration. For instance, in the work of Nakashima et al. [20], the performance of two energy technologies used for EOR, namely, the gas lifting and the two-phase screw pumping processes are compared in light of the exergoeconomy theory. Those results have been used in turn to calculate the cumulative exergy cost and the specific CO₂ emissions of different fuels, chemicals and transportation services [43] in petrochemical refineries, biorefineries [44], fertilizers complexes [45] and even of the Brazilian electricity mix [17]. The methodology used in those studies relies on the concept of the *Total Unit Exergy Cost* (c_T) [kJ/kJ], defined as the rate of exergy necessary to produce one unit of exergy rate (or flow rate) of a substance, fuel, electricity, work or heat comprised in the petroleum production platform. Analogously, the specific *CO₂ emission cost* (c_{CO_2}) [gCO₂/MJ] is defined as the rate of CO₂ emitted to obtain one unit of exergy rate (or flow rate) of the stream analyzed (either material or energy flow). Thus, by considering the control volume embodying each representative process unit of the offshore platform, the exergoeconomy balance of the total exergy costs can be written as in Equation (4):

$$\sum_j c_{T,P}^j \dot{B}_{T,P}^j = \sum_i c_{T,F}^i \dot{B}_{T,F}^i \quad (4)$$

where B stands for the exergy rate (or flow rate) of the exergy inputs (or fuels, F) and products (or byproducts, P) of the respective control volume. Similarly, the CO₂ emission cost balances can be written as shown in Equation (5), where the *net direct CO₂ emissions*, either produced by burning the fuel i consumed, or arisen/captured from/through other chemical reactions (for instance, chemical absorption), are accounted for in the $\dot{M}_{CO_2,F}^i$ and $\dot{M}_{CO_2,Rxn}$ terms [gCO₂/s], respectively:

$$\sum_j c_{CO_2}^j \dot{B}_{T,P}^j = \sum_i \left(c_{CO_2,F}^i \dot{B}_{T,F}^i + \dot{M}_{CO_2,F}^i \right) + \dot{M}_{CO_2,Rxn} \quad (5)$$

It is noteworthy that, in the case of the allocation of CO₂ emissions, initial input values for the specific CO₂ emissions must be considered equal to zero (or known). This differs from the conventional approach of adopting the unity (or a known value from previous analyses) as the unit exergy cost of an external input entering the control volume. Figures A.1-A.4 in Appendix A show the simplified control volumes adopted for calculating the unit exergy costs and specific CO₂ emissions related to the streams involved in the various configurations studied of the offshore petroleum platforms. Oftentimes practitioners use the specific power consumption (kWh/t_{crude oil}) or the overall energy intensity (MJ/t_{crude oil}) in order to quantify the performance of the offshore petroleum platforms and some of their components. However, the exergoeconomy approach is more advantageous as it allows mapping the generation of the costs along the industrial processes and, consequently, to spotlight the systems responsible for the highest exergy consumption and energy degradation, as well as those entailing the largest non-renewable CO₂ emissions. Furthermore, this methodology allows an improved insight into the influence of the energy demanding CO₂ capture, recompression and sequestration processes on the overall platform performance. This is possible thanks to an iterative calculation of the unit exergy costs and the specific emissions of the recirculated CO₂-rich streams sent to the well. Actually, they should be considered as platform products inasmuch as they aim to enhance the petroleum recovery, whereas mitigating the environmental impact.

4. Results and discussion

In the following sections, the performance of the four FPSO setups, i.e. two relying on the conventional SCGT system with and without an amine-based carbon capture system, and the other two using the oxyfuel S-Graz and Allam cycles, are compared in terms of (i) the specific exergy consumption, (ii) the net amount of CO₂ emissions, (iii) the exergy efficiency, (iv) the specific exergy destruction at plantwide and subunit-wise levels, as well as (v) the unit exergy cost and specific CO₂ emissions of the streams pertinent to each process unit.

4.1. Energy and exergy consumption remarks

Table 2 summarizes the main design parameters, some of which have also been reported in a specific basis. The oxyfuel configurations are the ones which consume the least amount of fuel in order to supply power and heat to the same basic petroleum processing units, with the Allam equipped platform burning 42-49% less fuel than any other configuration. Consequently, it is also the configuration which exports the most of methane-rich gas, as it is shown in the Table 2. This is still valid, despite the need of the Allam cycle-powered platform to burn an extra amount of fuel in an auxiliary boiler. This additional consumption is necessary to render feasible the primary separation of petroleum, as it will be evinced later by using the energy integration analysis.

The air intake conditions reveal how much air is necessary to control the combustion temperature. The oxyfuel cycles demand much less air intake due to the enrichment of the oxidant stream. Anyhow, the Allam cycle is still singular at this aspect, since its turbine technology combines both steam and gas turbine technologies in order to withstand the supercritical pressures and elevated temperatures. Therefore, although Allam cycle works at 200-400 bar, the turbine inlet temperature is conserved at 1100-1200°C. Moreover, there is a benefit to operate at such high pressures as it impacts the space and weight budget. In other words, the equipment required can be more compact and, as the working fluid already consists mostly of CO₂, the energy demand in the flue gas purification is reduced, e.g. lower parasitic power consumptions are achieved [30].

The relative advantage of oxyfuel cycles is the ease of separation between CO₂ and H₂O, two main products of combustion, since it can be done via water condensation. Since the S-Graz cycle is categorized as a water-based oxyfuel cycle (i.e. its working fluid is mostly water, 78%), the condensate is removed from the CO₂ stream in the intercooling steps of the CO₂ compression. On the other hand, the Allam cycle is a CO₂-based power cycle and, as it has already acceptable levels of water, which may vary greatly from operation to operation, an extensive water-CO₂ separation

process may be spared. At last, the amine-based configuration also has a knockout condensation process which occurs along with the CO₂ compression stages, so that lower water content can be accomplished in the CO₂ injected.

As for one of the main parameters of interest, the largest amount of CO₂ captured is in the platform equipped with an S-Graz cycle, although the captured carbon dioxide stream has the lowest CO₂ purity (94.20% mol). The S-Graz cycle is followed by the post-combustion-based configuration which, despite the fact of releasing significant amounts of CO₂ into the atmosphere through the purified gas, still manages to capture 3.40 kg/s of CO₂ at 98.90% mol purity. At last, the Allam cycle captures 2.25 kg/s of post-combustion CO₂, since this cycle has the lowest fuel consumption.

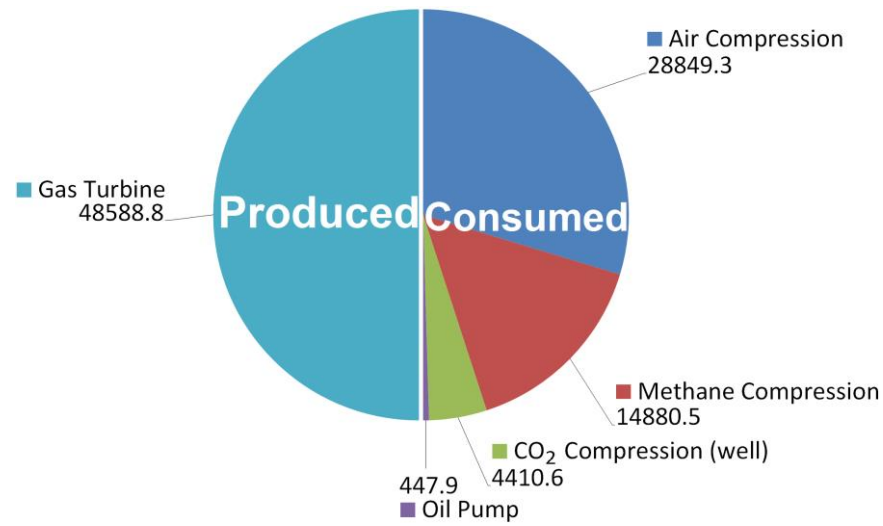
Table 2. Main process variables calculated for the four FPSO configurations with different CHP units and CCS approaches.

Process parameter	Platform layout with CHP unit and CCS approach			
	Conventional	Amine-based	S-Graz cycle	Allam cycle
Oil production flow rate (kg/s)	161	161	161	161
CO ₂ -rich stream from well (kg/s)	8.2	8.2	8.2	8.2
Methane fuel consumed (kg/s) ¹	1.62	1.74	1.53	0.88
Methane fuel consumed in aux. boiler (kg/s)	-	-	-	0.094
Specific methane fuel consumption (kg / ton oil) ²	10.09	10.85	9.48	6.07
Methane exported (kg/s)	26.38	26.25	26.47	27.02
Air consumption (kg/s)	63.03	67.76	31.38	19.40
Oxygen consumption (kg/s)	-	-	5.79	3.28
Oxygen purity (%)	-	-	99.5	99.5
ASU oxygen recovery (%)	-	-	79.19	79.19
ASU spec. power consumption (kWh/tO ₂)	-	-	286.3	286.3
ASU N ₂ rich waste gas (kg/s)	-	-	25.59	14.51
Combustor pressure (kPa)	4,000	4,000	4,000	30,000
Gas turbine exhaust pressure (kPa)	300	300	100	3,000
Turbine inlet temperature (°C)	1,150	1,150	1,400	1,150
Net power produced (kW) ³	19,739	21,231	27,477	27,238
Cooling requirement (kW) ⁴	28,367	60,815	52,169	22,627
Spec. cooling req. (kJ/toil)	176,193	377,733	324,031	140,540
Knockout cond. from CO ₂ compression (m ³ /h)	-	5.4	6.3	-
Combustor/Gas turbine steam splitting (%)	-	-	91.5/8.5	-
Recycled flue gas CO ₂ mole fraction	-	-	0.22	0.98
Percentage of recycled flue gas (%)	-	-	71.52	96.02
Oxyfuel cycle total water disposal (m ³ /h)	-	-	11.40	6.82
Min. temperature approach - flue gas/WHRU (°C)	-	-	83	5
Water/CO ₂ mixture flash pressure (kPa)	-	-	4	3,000
CO ₂ emissions within methane exported (kg/s)	2.06	2.05	2.07	2.11
CO ₂ captured (kg/s) ⁵	-	3.40	3.98	2.25
CO ₂ captured purity (% mol)	-	98.90	94.20	98.07
Spec. post-combustion CO ₂ captured (kgCO ₂ /toil) ⁵	-	21.1	24.7	14
Total CO ₂ emitted (kg/s)	4.23	1.14	2.3E-3	0.29
Amine loop make up water (m ³ /h)	-	3.6	-	-
CO ₂ recovery using MEA (%)	-	74.8	-	-
CO ₂ fed to amine loop (kg/s)	-	4.55	-	-

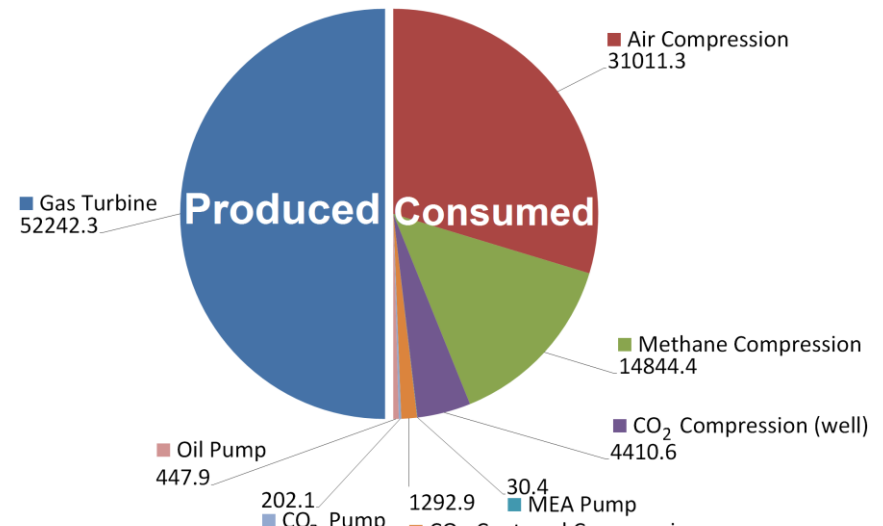
Process parameter	Platform layout with CHP unit and CCS approach			
	Conventional	Amine-based	S-Graz cycle	Allam cycle
Amine loop reboiler duty (kW)	-	17,012	-	-
Spec. desorber steam cons. (MJ/kg _{CO2})	-	4.99	-	-

(1) Fuel consumed in power cycle solely; (2) Calculation considering the total amount of fuel consumed in the platform, namely, the sum of fuel consumed in power cycle and fuel consumed in the auxiliary boiler; (3) Net power produced considering the *Power Generation Unit* control volume (in red in Figures 1-4); (4) Cooling tower water inlet at 18°C, 60% relative humidity; (5) This value only includes the CO₂ produced when burning the methane fuel, excluding the original CO₂ already extracted from the well, separated by membrane and reinjected.

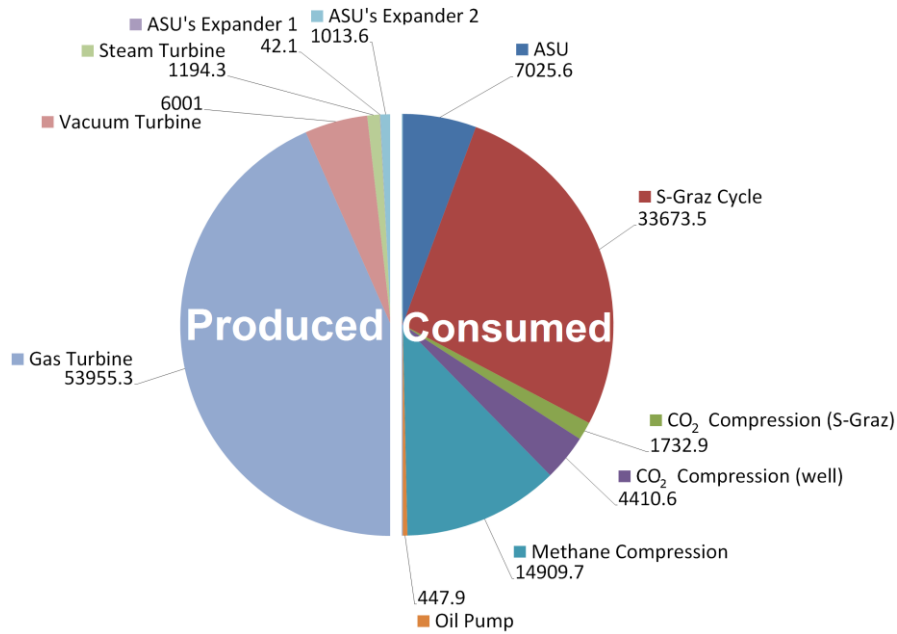
Figures 5a-d show the distribution of the consumption of power among the different consumers in the various designed setups. On both the conventional and the amine-based platform, the normal air compression system is responsible for about 59.4% of the consumption of the overall power generated (considering compressor and expander as separated modules). Meanwhile, in the oxyfuel configurations, the air compression at ASU consumes 11.30% and 12% of the total power generated in the S-Graz and Allam cycles, respectively. The exported gas compression is the second largest power consumer in all the plants considered, except for the Allam cycle-powered FPSO, in which the exported natural gas compression achieves 46% of all the power produced. Actually, in this configuration that figure surpasses by far the second most power-intensive process, namely the power generation unit itself as well as the air separation unit (12%). In contrast, the S-Graz internals (i.e. recycle compressors, pumps, and so forth) consume up to 54.14% of the power generated by the power cycle, whereas in the Allam cycle, its internal consumption responds for only 16% of the total power produced. The third largest consumption in the platforms, except for the S-Graz based configuration, corresponds to the compression process of the incoming CO₂ from the well to re-injection. The prominent positions occupied by the compression systems might be explained by the large mass flow rates of gas, and particularly elevated pressures for exporting to shore or re-injecting gas into the Pre-Salt region. It is important to emphasize that, due to the technical regulations of the offshore electricity generation in Brazilian platforms, no net power export is aimed, and thus, only the platform internal power demands need to be guaranteed. Finally, other ancillary processes represent up to 3.78%, 3.51%, 0.92% and 1% of the overall consumed power in the amine-based, S-Graz, conventional and Allam powered configurations, respectively.



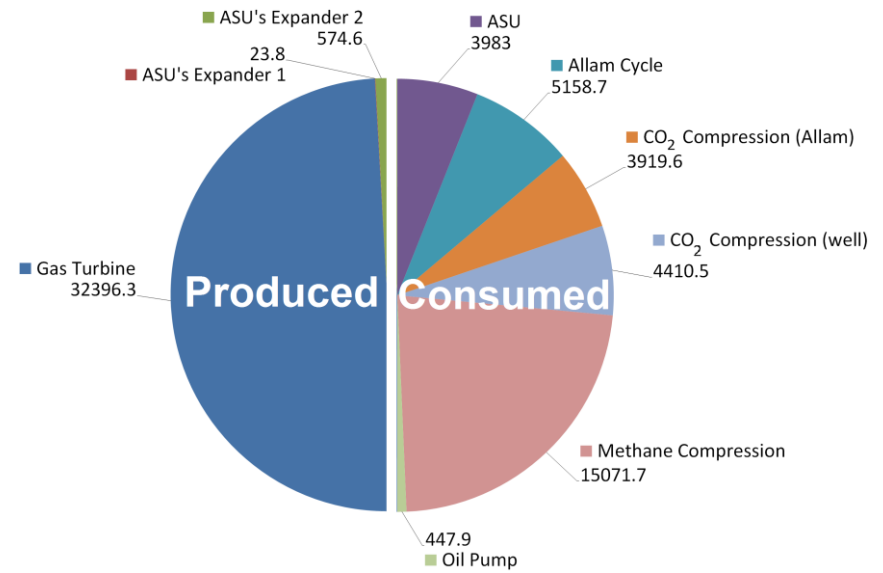
(a) Conventional



(b) Amine-based



(c) S-Graz cycle-powered



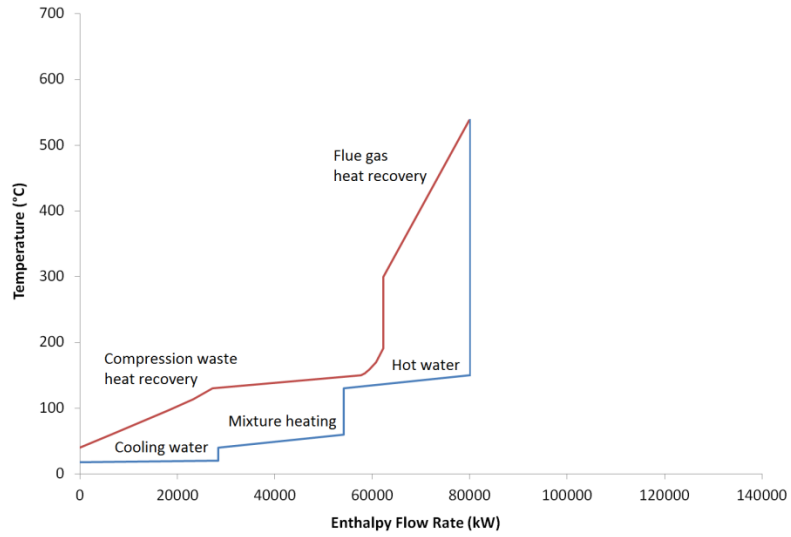
(d) Allam cycle-powered

Figure 5. Breakdown of the power supply and demand of (a)Conventional, (b)Amine-based, (c)S-Graz and (d)Allam cycle powered platforms (in kW).

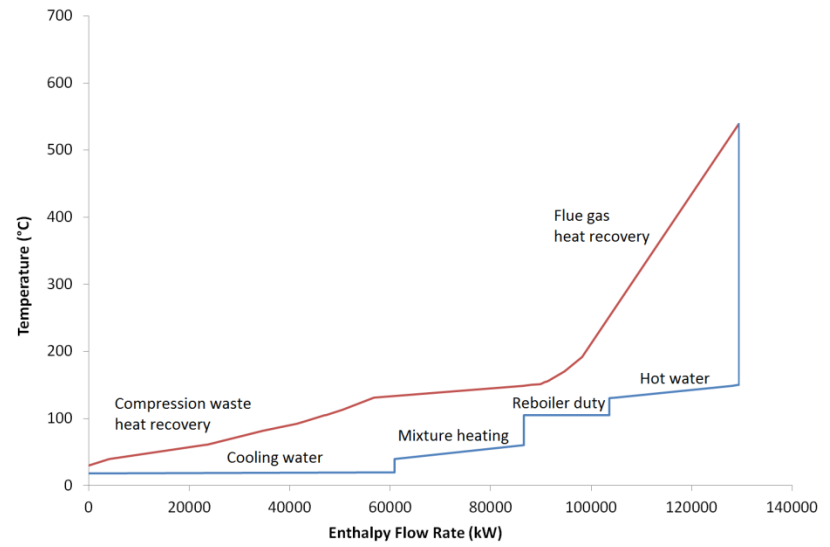
4.2. Energy integration analysis

The energy integration method provides means for calculating the minimum energy requirement (MER) of a chemical and cogeneration production plant. This approach allows to prioritize the recovery of the waste heat available throughout all the energy conversion systems over the utilization of costly and high temperature energy resources, such as valuable natural gas [46]. According to this, an energy integration analysis was carried out in order to determine whether the recovery of the waste heat available along the unitary operations of the platform might reduce the amount of fuel consumed, by either preheating the boiling feed water or raising the steam required in the process, otherwise provided by an auxiliary boiler. To this end, supply and target temperatures of the streams are collected along with the respective heat duty. Next, based on the particularities of the heat transfer process, adequate temperature differences are chosen. A global approach of 20 °C is considered whenever the minimum temperature differences are not specified. Particularly tight minimum temperature differences are selected (2-5°C) in the case of the air liquefaction process and the vapor compression refrigeration system, as heuristically suggested. Henceforth, the energy integration method is applied to build a temperature-enthalpy flow rate ($T-H$) composite curve that elucidates the minimum hot (fuel burnt in auxiliary boilers) and cold utility (cooling water) consumptions.

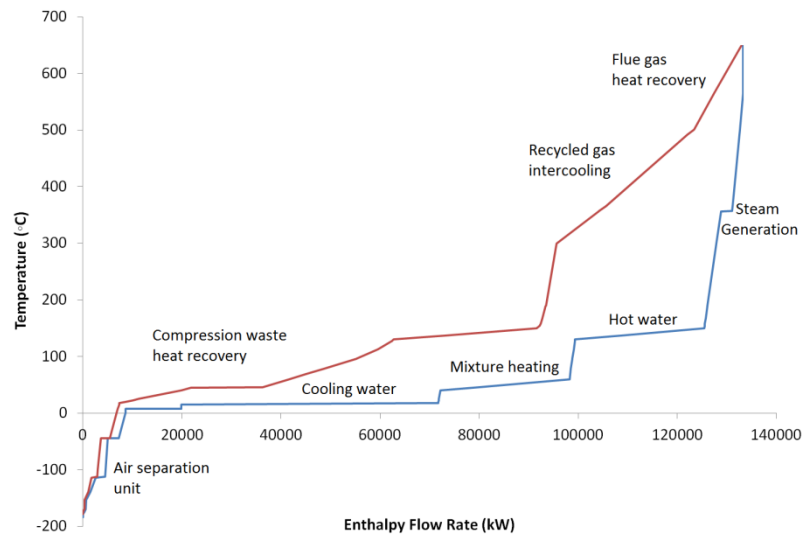
Figures 6a-d show the composite curves of the four studied FPSO configurations, which already include the utility systems. According to these figures, with three of the four configurations (Fig. 6a-c), it would be theoretically possible to meet the minimum heating requirements of the platform by recovering the waste heat throughout the overall facility, without the need of burning an extra amount of fuel in an auxiliary boiler. The only exception is the Allam cycle-powered platform. This is in agreement with the findings of Allam et al. [31] in which a need for an external heat source at about 100-400°C is reported in order to balance the highly integrated heat requirements in the multiple stream heat exchanger (see Figure 4). According to the authors, this requirement is supposedly owed to the difference in the heat capacity of the CO₂-rich streams at 300 and 30 bar [30]. The outsourced heat requirement might be supplied either by an auxiliary boiler or by recovering the waste heat elsewhere in the plant, such as in the compression intercooling, or more specifically, from the compressors of the air separation unit. Despite the fact that some waste heat can be harnessed from the oxygen compression intercooling to meet the MER of the recycled flue gases and the oxidant stream, the energy requirement of the primary separation of petroleum must still be partially satisfied by using an auxiliary boiler, since there it not enough waste heat available at satisfactory temperatures elsewhere in the plant. It is also worthy to notice that the composite curves of the advanced configurations progressively become closer, decreasing the gap between hot and cold composite curves. This fact may suggest lower rates of exergy destruction due to reduced driving forces in the heat transfer processes. Eventually, the excess waste heat that is not recovered is dissipated by using a cooling water system. The respective cooling requirement for each configuration in Figure 6 has been indicated in Table 2.



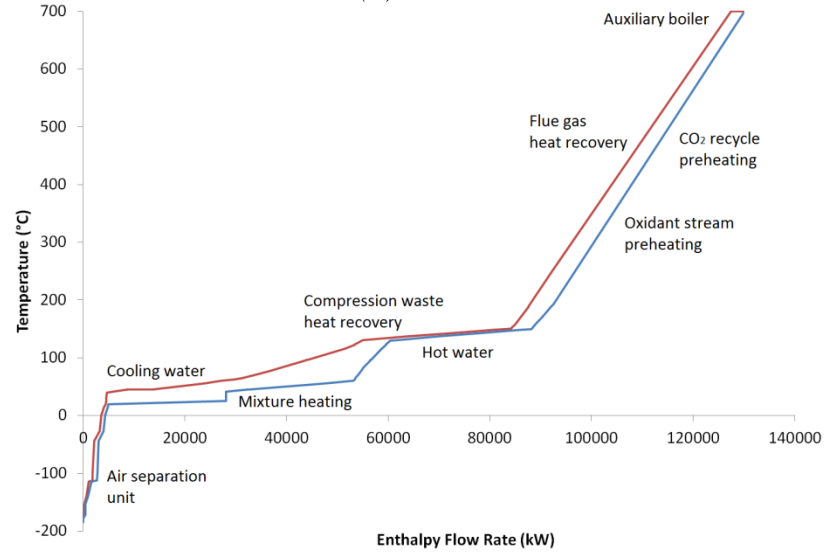
(a) Conventional



(b) Amine-based



(c) S-Graz-cycle powered



(d) Allam cycle powered

Figure 6. Composite curves for (a)conventional, (b)amine-based, (c) S-Graz and (d) Allam cycle powered platforms.

4.3. Exergy destruction and exergy efficiency

The closer a process is to be completely reversible (internally and externally), the lesser the exergy destroyed. However, real processes take place at finite-driving forces and, thus, they are inherently irreversible. Accordingly, the exergy analysis gives a means to measure and allocate such irreversibility, accounted for in the amount of exergy destruction, so that the processes with the worst exergy performance can be identified and means to minimize the exergy destruction can be envisaged. This analysis considers a dead state temperature and pressure at $T_0=25^\circ\text{C}$ and $P_0=101.3\text{ kPa}$, respectively. Another indicator which can be closely related to the exergy destruction is the exergy efficiency. Multiple definitions of exergy efficiency are available in the literature and others could be developed in order to assess certain aspects of the studied system.

Figure 7 shows the overall exergy efficiencies as defined in Table 1, used to rank the performance of the platform layouts. It must be noticed that, as the oil virtually goes unchanged through the control volume after the primary separation is performed, it carries with it a large amount of transit exergy. Therefore, if its absolute chemical exergy were to be included in the efficiency calculation, the results may lead to untruthfully large exergy efficiencies, misrepresenting the performance of the actual transformations occurring inside the platform. The same arguments would apply for the large absolute exergy flow rate of the methane-rich exported gas, compared to the much lower amount of the absolute exergy of the gas fuel, consumed to drive the compressors. As for the conventional and post-combustion configurations, it is noticeable a sharp platform-wide efficiency drop. This reduction is expected, given that the amine-based setup is the same as the conventional one alongside an amine loop and a CO_2 compression process (see Figures 1 and 2). Thus, even though the power and heat demands of the processing plant are the same; more fuel must be burnt in the amines-based layout, so that the energy demand of the additional units (solvent pumps, cooling and heating requirements, and compression units) is satisfied (see Table 2). So according to Equation (1), the increase in \dot{B}_{fuel}^{CH} causes a *power* exergy efficiency drop of roughly 2 percentage points in the chemical absorption-based layout compared to the conventional configuration. The same logic applies when considering the *cogeneration* exergy efficiency definition, which suffers a similar drop. At last, when considering the *separation* exergy efficiency definition in the amines-based FPSO, the gain in exergy of the pressurized CO_2 captured and the exported products naturally do not outweigh fuel exergy consumed due to the compression irreversibility. This fact results in a sharp drop in *separation* efficiency compared to the conventional configuration.

Meanwhile, the reduction in the S-Graz fuel consumption raises both the power and cogeneration efficiency of the plant. This increase in efficiency might be explained by the higher temperatures that oxyfuel turbomachinery is able to withstand and the layout of the cycle itself. Actually, this arrangement seeks to recover energy from high temperature gases and convert it into more power in a steam turbine (see Figure 3). The S-Graz *separation* efficiency is still significantly lower than in the conventional setup, but it is slightly higher than in the amines-based setup, according to Figure 7. Actually, although the S-Graz cycle requires less fuel to function (see Table 2), it destroys more exergy than the conventional open cycle (see Figure 8) due to additional energy conversion stages. Moreover, in the conventional FPSO, a large amount of stack gases are released when they are still at high temperature (approx. 300°C), entailing a partially avoidable exergy destruction.

Finally, the Allam cycle seems to be the most advantageous among all the power cycles studied. This power cycle consumes the least amount of fuel for the sake of supplying the combined power and heat to the processing plant and the power auxiliary loads. As a consequence, the power and cogeneration efficiencies sharply increase, becoming 20% higher

than the efficiencies of the other power generation cycles. The extensive usage of heat integration displayed in its composite curves, as well as the discussed characteristics of its working fluid, composed of nearly pure CO₂, warrants superiority of Allam cycle in this aspect. As for the *separation* efficiency, the Allam cycle-powered platform outperforms the other two advanced configurations, but it is still quite lower than in the conventional configuration.

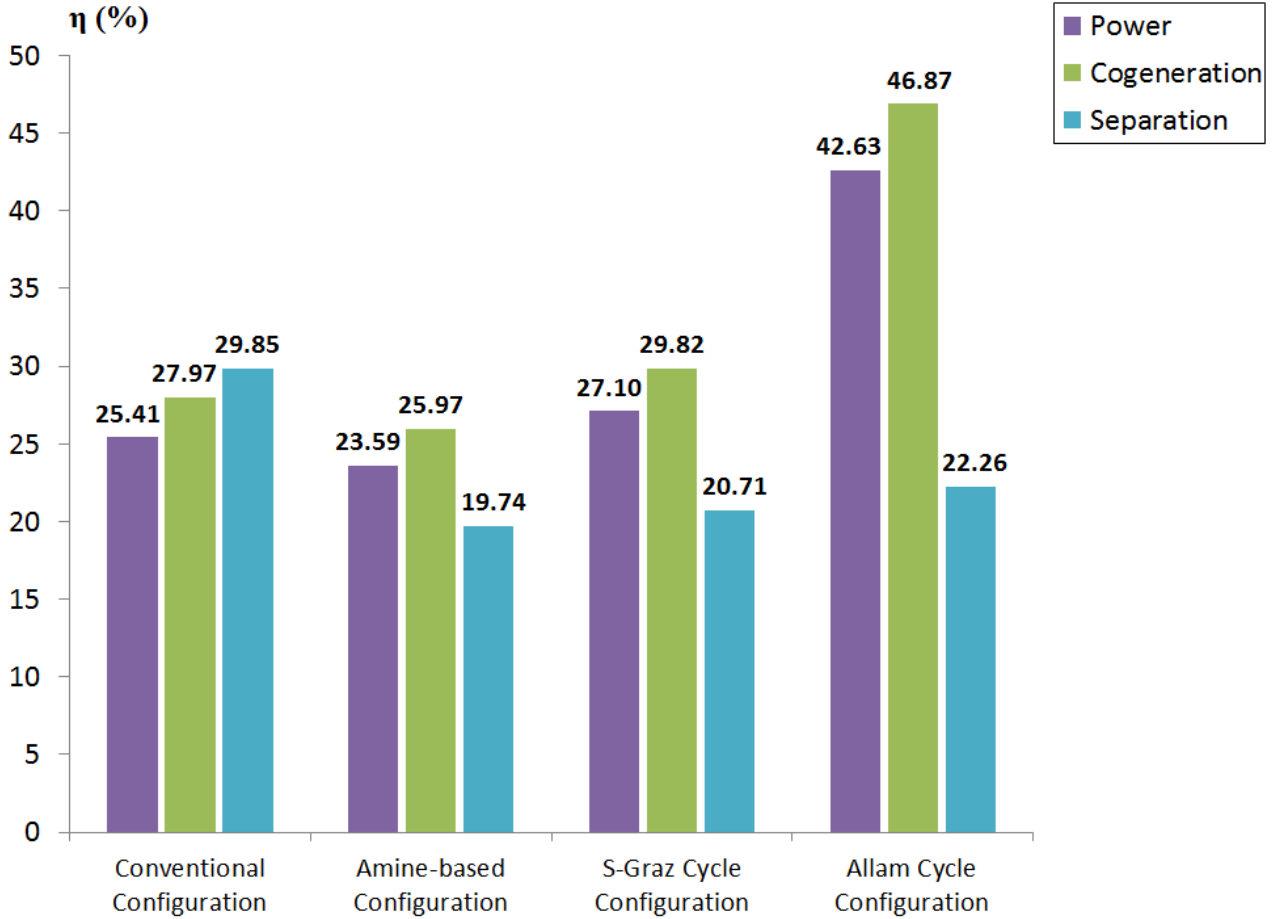


Figure 7. Exergy efficiencies calculated at the platform-wide (separation) and utility system levels (power, cogeneration).

Remarkably, the energy conversion processes that impact the most the oxyfuel cycles efficiency is the air separation unit (ASU). Although the ASU efficiency is in accordance with energy consumption estimates in open literature [47], some measures can be taken to improve upon its performance. The reversible work consumed by the ASU corresponds to the minimum exergy necessary to separate the air into its main components (namely, oxygen and nitrogen-rich streams). However, since the real system operates irreversibly, the actual work is indeed much higher. The actual exergy consumed per ton of oxygen produced is calculated as 286.3 kWh/tO₂, which is within the range (280-340 kWh/tO₂) reported in the literature for typical ASUs [48]. Equation (6) shows the definition considered to calculate the standalone ASU exergy efficiency:

$$\eta_{ASU} = \frac{\dot{W}_{sep. consumed, reversible}}{\dot{W}_{sep. consumed, actual}} \quad (6)$$

By using this definition, an exergy efficiency of 17.68% can be calculated. This performance can be further improved by better integrating the dual pressure columns via pump around

systems and intermediate heat exchange sections in the LPC. In this way, the temperature differences are lowered, while further decreasing the associated exergy destruction. Another way to achieve the same goal is to use heat-integrated distillation (HIDiC) columns [49]. These columns are partially embedded one into another in order to provide a more extended heat exchange area. Lower pressures and better temperature approaches in the contact columns, as well as better condenser/reboiler integrations can also improve the ASU performance. Thus, further research must still be conducted for this particular case.

An alternative way of comparing the performance of the different setups is through the specific exergy destruction per ton of exported oil. This measure can be directly linked to others, such as the specific consumption, presented in Table 2. Figure 8 is in agreement with other metrics, especially in the case of the Allam cycle-powered configuration. As expected, the most efficient power cycle (considering the power and cogeneration exergy efficiencies) destroys the least amount of exergy. The results in Figure 8 are also in accordance with the performance indicators found for the amine-based configuration. As the least efficient plant, it stands to reason that the amines-based platform would also destroy the largest amount of exergy. The Allam cycle-powered platform destroys nearly 40% less exergy than the conventional configuration, and around 48% less than the chemical absorption-based concept.

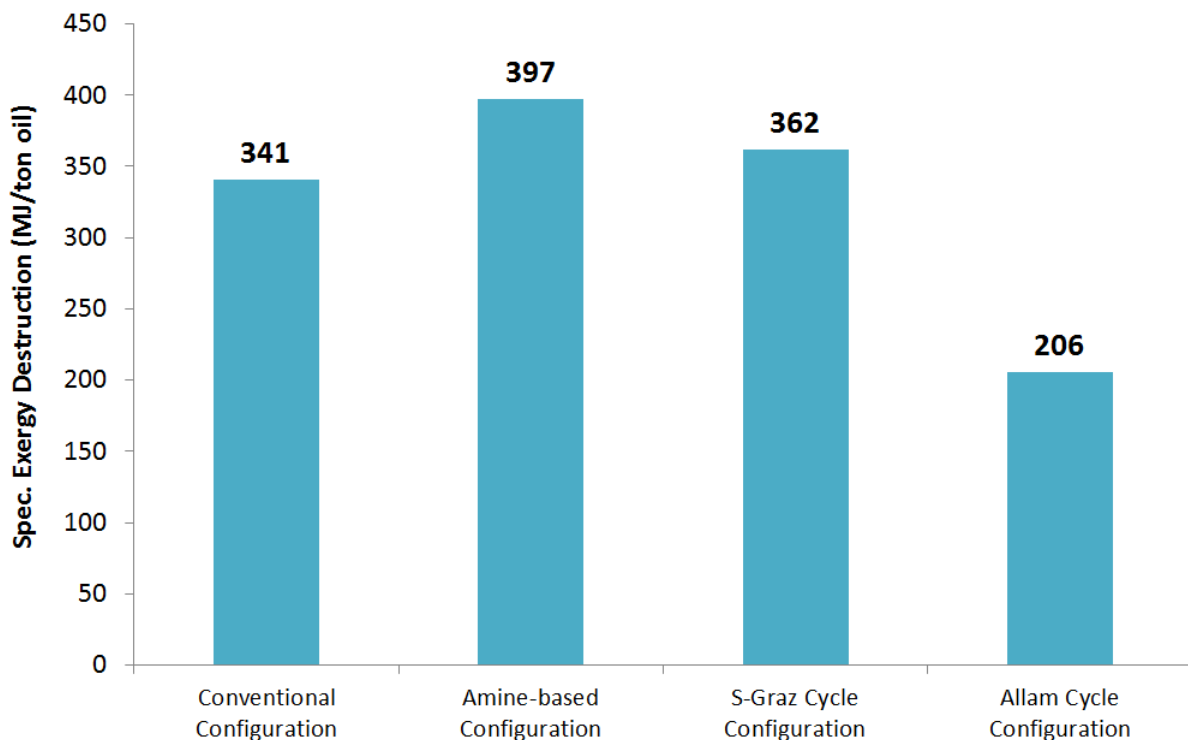


Figure 8. Specific exergy destruction (MJ/t oil) for the four platform configurations using conventional and advanced power generation systems with carbon capture approaches.

Furthermore, since the main objective of this investigation about advanced cogeneration plants for offshore platforms is precisely achieving an extensive mitigation of the atmospheric effluents, the specific CO₂ emissions are also summarized in Figure 9. Evidently, a dramatic cutdown of the CO₂ emissions can be achieved by employing the advanced configurations. In this way, the massive environmental impact of the CO₂ discarded by the conventional platforms may be attenuated by tenfold to 1000 times. Moreover, the amine-based and Allam cycle-powered platform discharges 100 times more CO₂ than the S-Graz setup due to the release of the purified gas resultant of the limited capacity of monoethanolamine CO₂ sequestration, as well as of the discharge of CO₂ from the Allam cycle through the CO₂-containing condensate along with the CO₂ resultant from the burning of extra fuel in the auxiliary boiler.

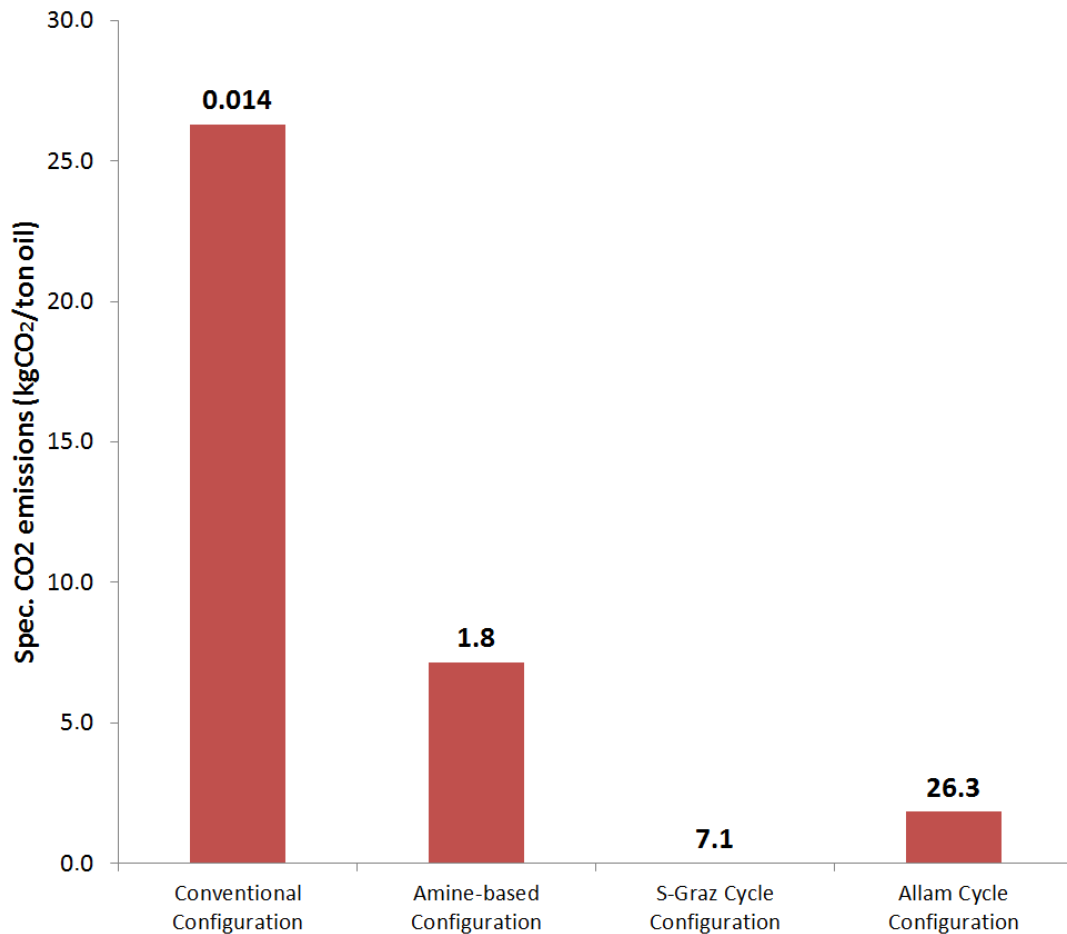


Figure 9. Specific CO₂ emissions (kgCO₂/t_{oil}) for the four platform configurations using conventional and advanced power generation systems with carbon capture approaches.

Finally, an exergy destruction breakdown helps elucidating which subunits composing the offshore petroleum platforms exhibit the highest rates of exergy destruction. This kind of portrayal sheds light upon which processes and components are the main candidates for potential improvements in their operation parameters or even for substitution and revamping. Figure 10 shows that the power generation systems, encompassing the OCGT system with the bottoming waste heat recovery unit (WHRU), and the S-Graz combined power and heat production, entail the largest contributions to the exergy destroyed in all four platforms, corresponding to 68.17%, 60.35%, 48.67% and 56.64% for the conventional, amine-based, S-Graz and Allam cycle-powered configurations, respectively. This can be explained by the fact that in this part of the platform the highly irreversible combustion reactions take place, in which about 25-30% of exergy is destroyed [50]. The energy intensive petroleum separation, which takes place at large temperature differences, contributes to a large share of exergy destruction [39, 51], ranging from 9.29 to 20.74%. The units enclosing the processes characteristic to the oxyfuel or chemical absorption units, namely the air separation unit and the amine loop, follow the primary separation as the most exergy-destructive processes. For instance, the CO₂ purification via chemical absorption is responsible for 14.47% of the exergy destruction. At the same time, the ASU stands for 8.63% of the exergy destruction in the S-Graz-powered platform, whereas in Allam cycle-powered platform this value amounts 8.61%. As it was shown in Figure 5, the compression processes are energy intensive as they manage large mass flows. By doing an exergy breakdown, the full picture emerges, and the most energy intensive processes are not necessarily the most exergy-intensive as well. As shown in Figure 10, in most

of the cases, these compression units do not represent but less than 5% of the exergy destruction in the platform. Other ancillary equipment, such as the heat exchange network and pressure drops devices account for the remaining exergy destruction. Notably, in the S-Graz cycle-powered layout, this number is over 20%, as it is the power cycle with the major number of additional equipment. The Allam cycle-powered setup upholds the lowest percentage of ancillary exergy destruction (4.36%), evidenced by its higher levels of energy integration.

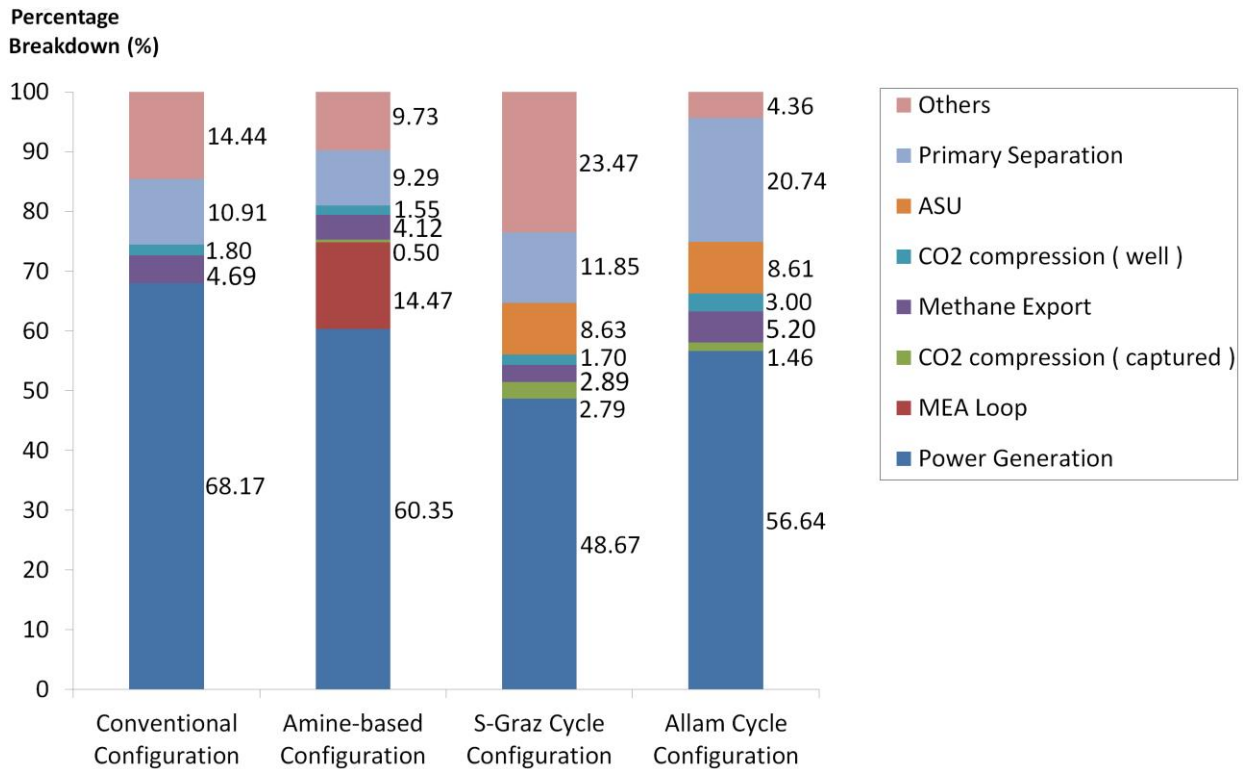


Figure 10. Exergy destruction breakdown for the four platform configurations using conventional and advanced power generation systems with carbon capture approaches.

4.4. Unit exergy cost and specific CO₂ emissions

By using the exergoeconomy analysis and a set of auxiliary criteria for exergy costs allocation (see Table A.5 in Appendix A), it is possible to track how each stream varies its specific CO₂ emissions and exergy expenditure as it goes through the different energy conversion systems. As the main exported products, Figure 11 shows the calculated values for the unit exergy costs and specific CO₂ emissions of the crude oil and natural gas.

Clearly, the highest environmental impact corresponds to the conventional scenario, in which 2.57 gCO₂ are emitted per unit of exergy (MJ) of natural gas exported, in contrast with the strikingly three to tenfold lower (0.25-0.85 gCO₂/MJ) emissions produced by using the more advanced setups (i.e. amine-based, S-Graz and Allam cycle-powered platforms). Meanwhile, the difference in the unit exergy costs of the crude oil produced is less pronounced between all the scenarios, although the highest specific CO₂ emissions are still attributable to the conventional configuration. More detailed information about the physical and thermodynamic properties, as well as the unit exergy costs and specific CO₂ emissions of selected streams for each configuration of offshore platform are shown in Figs. A.1 - A.4 and in Tables A.1 - A.4 in Appendix A. For instance, oxygen production in both oxyfuel-based setups have a similar unit exergy cost, but it nearly doubles the cost of the heat exergy fed to the reboiler in the amine loop. The strikingly different CO₂ emissions costs of the streams leaving the S-Graz cycle-powered platform is a consequence of the hundredfold less CO₂ emissions produced compared to the Allam cycle-powered platform.

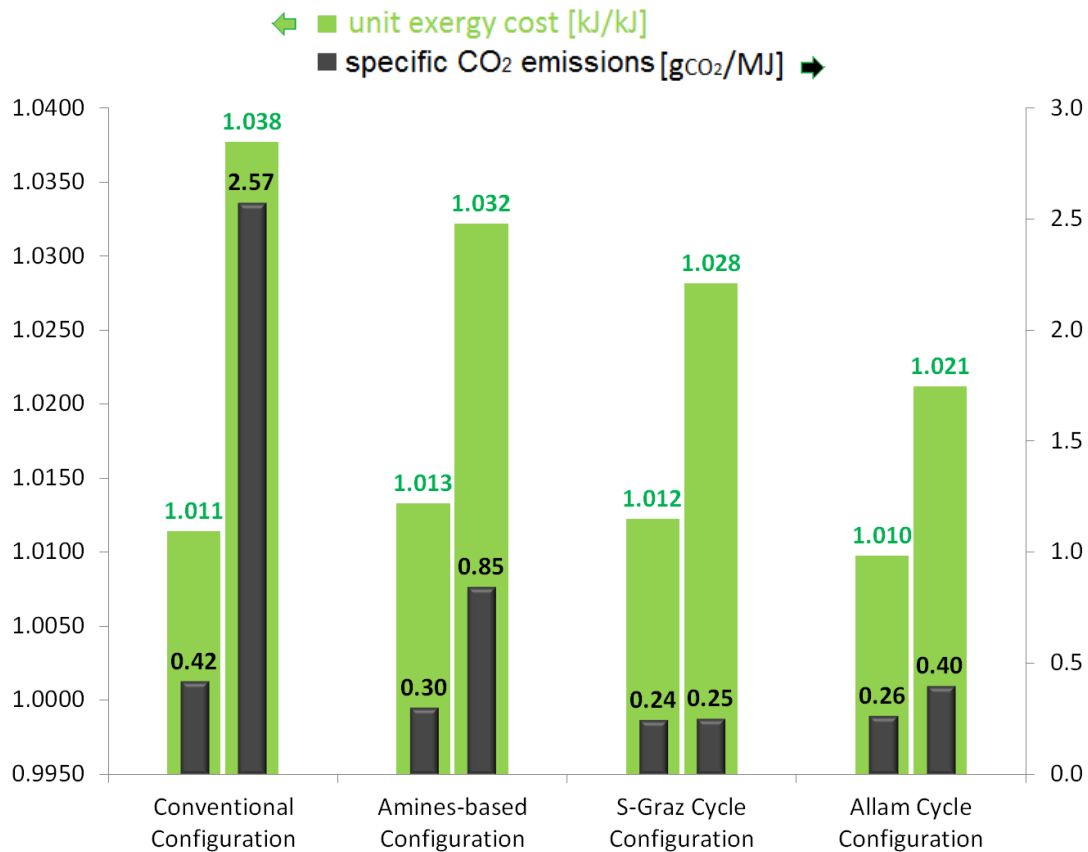


Figure 11. Unit exergy costs and specific CO₂ emissions of the crude oil and natural gas produced on the four platform layouts using conventional and advanced power generation systems with carbon capture approaches

5. Conclusions

The utilization of a simple gas turbine system in the utility systems of a conventional FPSO is, for the first time, compared with the integration of more advanced cogeneration cycles and carbon capture units, such as a chemical CO₂ absorption unit, an S-Graz cycle, and an Allam cycle, in terms of both exergy and environmental performance. The advanced configurations outperform both the conventional and chemical absorption-based utility systems in terms of the environmental impact, and the *power* and *cogeneration* efficiency definitions. In fact, the S-Graz-powered platform particularly mitigates nearly all the emissions, while achieving slightly higher *power* and *cogeneration* efficiencies than the conventional scenario. As for the scenario in which the platform is equipped with an amines-based post-combustion CCS unit, the energy intensive flue gas purification process demands more fuel to drive the ancillary CCS equipment. Consequently, the *separation* (platform) efficiency drops on all fronts and the extent of CO₂ mitigation still falls short in comparison to the oxyfuel cycles.

The platform integrated to the Allam cycle proved to be the most efficient at converting fuel exergy into power. On the other hand, the Allam cycle does not count on enough waste heat at an appropriate temperature to fulfil all heating requirements by only recovering waste heat along the platform, rendering an auxiliary boiler necessary to supply the heat duty to the petroleum primary separation. For that reason, the Allam cycle-powered platform fails to be less pollutant than the S-Graz cycle scenario. Another difference between the oxyfuel cycles is their very distinct operation parameters. While the S-Graz cycle operates at higher turbine inlet temperatures (1400°C) and moderate pressures (40 bar), the Allam cycle operates at moderate gas turbine temperatures (1150°C) and supercritical pressures (300 bar). Furthermore, both S-Graz and Allam cycles are categorized in distinct groups of oxyfuel cycles based on the

composition of their working fluids. Higher pressures in Allam cycle and its working fluid allow for more compact equipment, although advanced cycles require larger number of components than in the existing utility plants in FPSOs, which could make them prohibitively heavier and bulkier. In order to tackle this problem, centralized power stations (*power hubs*) hubs that supply power to a cluster of FPSO units operating in the same production field could be a more productive use of such power cycles. Thermodynamic analyses as well as viability studies about this alternative are currently under way [52]. Moreover, as long as other oxygen production methods cannot provide the same level of purity and large throughputs as in the cryogenic distillation process, further improvements can be expected from the use of heat-integrated distillation columns (HIDiC) and other modifications in the operation conditions and layout of the ASUs. Additionally, due to the unavoidable exergy destruction in the combustion processes, lower driving forces associated to narrower temperature differences in the heat recovery network may help reducing the amount of irreversibility in the petroleum production facilities. Moreover, the use of the exergy concept for rationally allocating the cumulative exergy consumption and the specific CO₂ emissions among the various intermediate and final products of the platform allows mapping the largest sources of exergy destruction and the process of the exergy costs formation.

Finally, it is fundamental to highlight that although CCS might be regarded as a promising and even necessary technique in the transitional period to a decarbonized future [4, 53]; many issues concerning these techniques still need to be addressed. Time necessary for proper development, security of carbon storage, public acceptance, and how it might stray investment from renewable energy, thus allowing for extended use of fossil fuels, and the factoring into the already tight carbon global budget are some issues called into question [53-55]. It is already known that most fossil fuel reserves should remain unexploited if global warming below 2°C is to be achieved [56]. It follows that carbon capture, if implemented, should be used towards taking out carbon from the already carbon loaded atmosphere, instead of being used to further extract hydrocarbons that will, in turn, require even more effort to mitigate.

Acknowledgments

The present work was supported by the National Agency of Petroleum, Natural Gas and Biofuels (ANP) and Shell Brazil, through the Investment in Research, Development and Innovation Clause, contained in contracts for Exploration, Development and Production of Oil and Natural Gas. The third author would like to acknowledge the National Agency of Petroleum, Gas and Biofuels – ANP and its Human Resources Program (PRH/ANP Grant 48610.008928.99), and the Colombian Administrative Department of Science, Technology and Innovation – COLCIENCIAS. Fourth author would like to thank National Research Council for Scientific and Technological Development, CNPq (grant 304935/2016-6).

Appendix A

Tables A.1 - A.4 summarize the physical and thermodynamic properties, as well as the unit exergy costs and specific CO₂ emissions of selected streams for each configuration of offshore platform shown in Figures A.1 - A.4. As it can be seen, both the heat exergy supplied (e.g. primary separation heating requirement and reboiler duty) and the overall power generated have the highest unit exergy costs and specific CO₂ emissions associated, thus, directly impacting the processes that depend on those utility streams. Actually, this effect can be readily evidenced from the exergy intensity and the environmental impact calculated for the products of the air separation unit (e.g. oxygen) and the CO₂ compression trains. This also holds for the utility streams supplied in the form of heat exergy to the carbon capture unit and the primary separation processes.

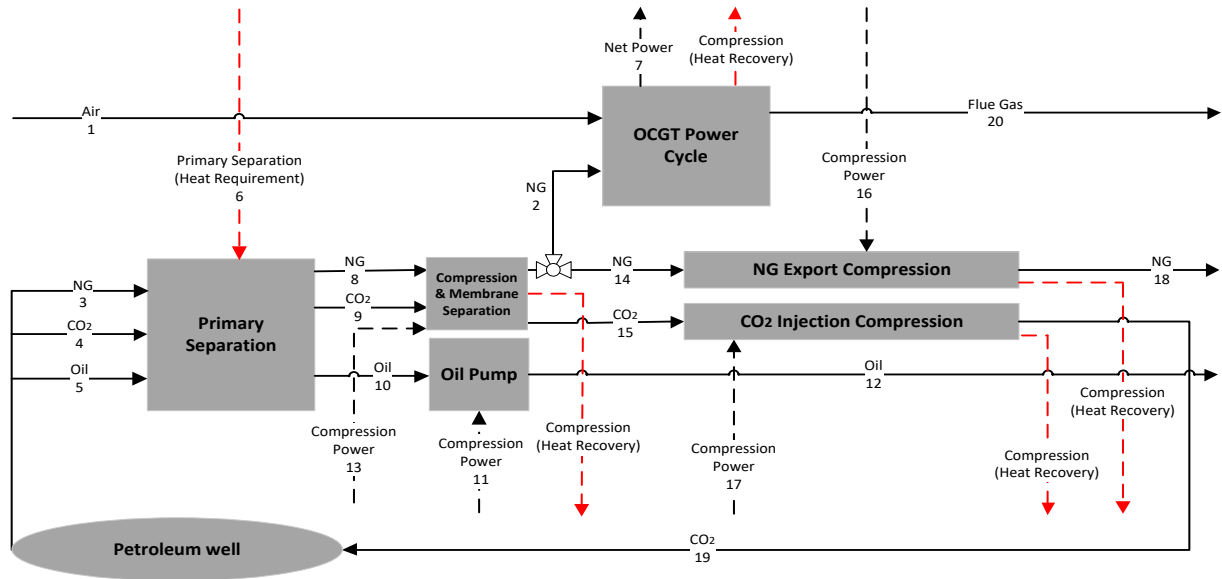


Figure A.1. Conventional offshore platform. Calculation scheme for the unit exergy cost and specific CO₂ emissions.

Table A.1. Thermodynamic properties and exergy cost of selected streams in Fig A.1, Conventional offshore platform.

N°	Name	T (°C)	P (kPa)	m (kg/s)	B _T (kW)	c (kJ/kJ)	c _{CO2} (gco ₂ /MJ)
1	Combustion air	25	101.3	63.0	0.0	1.0000	0.00
2	Natural gas (fuel)	38	4,800	1.6	78,572	1.0235	1.38
3	Natural gas (well)	40	1,500	28.0	1,349,493	1.0083	0.32
4	CO ₂ (well)	40	1,500	8.2	63,442	1.0083	0.32
5	Oil (well)	40	1,500	161.0	7,211,029	1.0083	0.32
6	Primary separation (Heating requirement)	150	-	-	1,985	12.5183	360.42
7	Net power (to compression systems)	-	-	-	1,9739	3.3538	219.61
8	NG to compression & membrane	40	1,500	28.0	1,349,493	1.0112	0.40
9	CO ₂ to compression & membrane	40	1,500	8.2	61,856	1.0112	0.40
10	Oil to pump	60	1,500	161.0	7,211,029	1.0112	0.40
11	Oil pump power	-	-	-	447	3.3538	219.61
12	Oil export to shore	60	2,300	161.0	7,211,029	1.0114	0.42
13	Gas compression power	-	-	-	8,039	3.3538	219.61
14	Methane-rich exported natural gas	38	4,800	26.4	1,276,307	1.0235	1.38
15	CO ₂ rich-permeate	38	300	8.2	60,975	1.0235	1.38
16	NG export compression power	-	-	-	7,793	3.3538	219.61
17	CO ₂ compression power to injection	-	-	-	3,458	3.3538	219.61
18	Natural gas export	113	24,500	26.4	1,281,524	1.0377	2.57
19	CO ₂ (from well) to injection	130	45,000	8.2	63,442	1.1332	11.11
20	Flue gas	300	300	64.7	11,753	0.0000	0.00

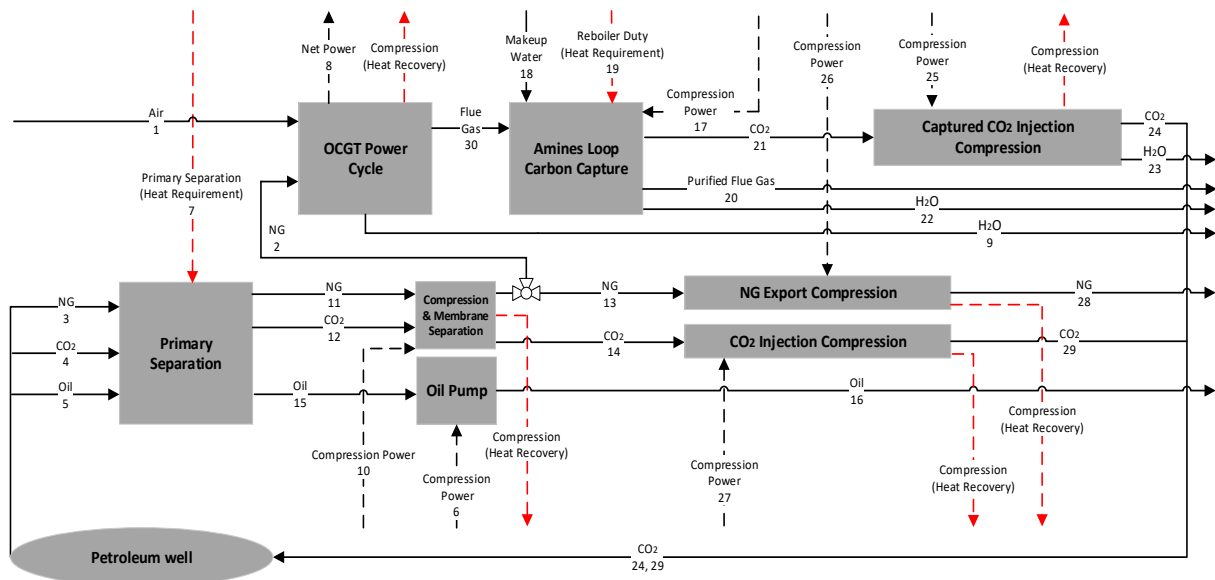


Figure A.2. Offshore platform with a chemical absorption carbon capture unit. Calculation scheme for the unit exergy cost and specific CO₂ emissions.

Table A.2. Thermodynamic properties and exergy cost of selected streams in the Fig A.2. Offshore platform with a chemical absorption carbon capture unit.

N°	Name	T (°C)	P (kPa)	m (kg/s)	B ^T (kW)	c (kJ/kJ)	c _{CO2} (g _{CO2} /MJ)
1	Combustion air	25	101.3	67.8	0	1.0000	0.00
2	Natural gas (fuel)	38	4,800	1.7	84,490	1.0221	0.54
3	Natural gas (well)	40	1,500	28.0	1,349,493	1.0108	0.28
4	CO ₂ (well)	40	1,500	8.2	61,856	1.0108	0.28
5	Oil (well)	40	1,500	161.0	7,211,029	1.0108	0.28
6	Oil pump power	-	-	-	447	2.6014	56.10
7	Primary Separation (Heating requirement)	150	-	-	1,985	9.9620	58.15
8	Net power (to compression systems)	-	-	-	21,231	2.6014	56.10
9	Waste water	40	300	2.6	133	0.0000	0.00
10	Gas compression power	-	-	-	8,039	2.6014	56.10
11	Natural gas to compression & membrane	40	1,500	28.0	1,349,493	1.0131	0.29
12	CO ₂ to compression & membrane	40	1,500	8.2	61,856	1.0131	0.29
13	Methane-rich exported natural gas	38	4,800	26.3	1,270,456	1.0221	0.54
14	CO ₂ rich-permeate	38	300	8.2	60,975	1.0221	0.54
15	Oil to pump	60	1,500	161.0	7,211,029	1.0131	0.29
16	Oil export to shore	60	2,300	161.0	7,211,029	1.0133	0.30
17	Amine loop power consumption	-	-	-	30	2.6014	56.10
18	Makeup water	25	130	1.0	49	1.0000	0.00
19	Reboiler duty (Heating requirement)	104	-	-	3,566	9.9620	58.15
20	Purified flue gas	30	300	63.0	5,987	0.0000	0.00
21	Captured CO ₂ to compression	42	100	3.6	1,488	13.9292	69.36
22	Waste water	42	100	1.4	71	0.0000	0.00
23	Waste water	40	multiple	1.2	30	0.0000	0.00
24	Captured CO ₂ to injection	90	45,000	3.4	2,439	9.6762	67.31
25	Captured CO ₂ injection compression power	-	-	-	1,495	2.6014	56.10

26	NG export compression power	-	-	-	7,756	2.6014	56.10
27	CO ₂ (well) to injection compression power	-	-	-	3,458	2.6014	56.10
28	Natural gas export	113	24,500	26.3	1,275,577	1.0322	0.85
29	CO ₂ (from well) to injection	130	45,000	8.2	63,442	1.0983	3.02
30	Flue gas	40	300	66.9	6,925	1.0220	0.54

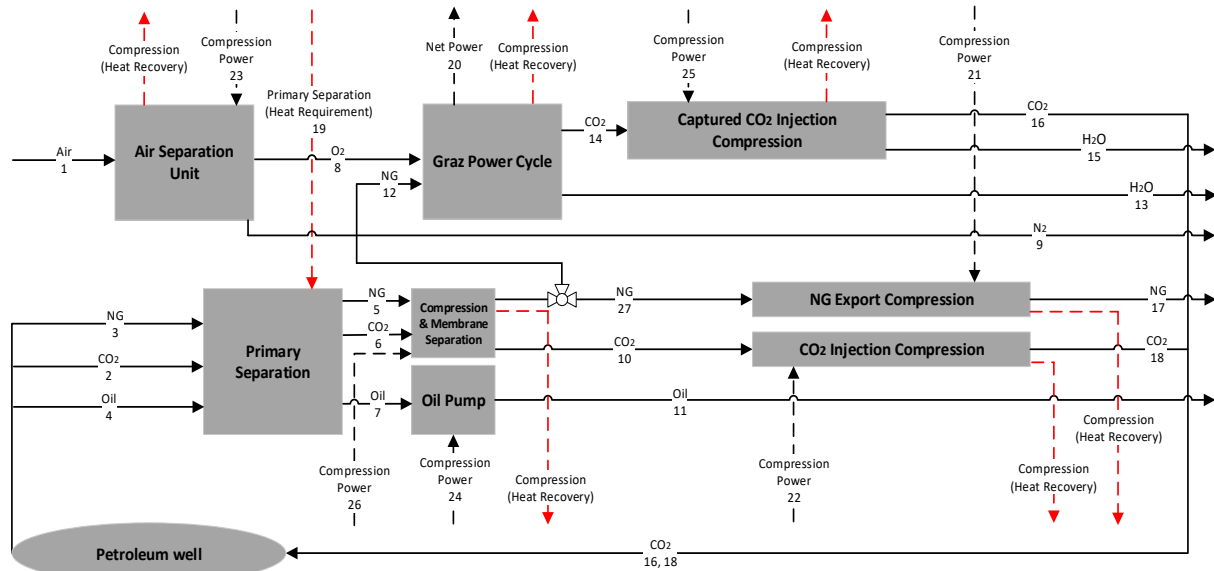


Figure A.3. Offshore platform integrated to an S-Graz power cycle. Calculation scheme for the unit exergy cost and specific CO₂ emissions.

Table A.3. Thermodynamic properties and exergy cost of selected streams in the Fig A.3. Offshore platform integrated to an S-Graz power cycle.

N ^o	Name	T (°C)	P (kPa)	m (kg/s)	B ^T (kW)	c (kJ/kJ)	c _{CO2} (g _{CO2} /MJ)
1	Combustion air	25	101.3	31.4	0	1.0000	0.00
2	CO ₂ (well)	40	1,500	8.2	61,856	1.0084	0.24
3	Natural gas (well)	40	1,500	28.0	1,349,493	1.0084	0.24
4	Oil (well)	40	1,500	161.0	7,211,029	1.0084	0.24
5	NG to compression & membrane	40	1,500	28.0	1,349,493	1.0121	0.24
6	CO ₂ to compression & membrane	40	1,500	8.2	61,856	1.0121	0.24
7	Oil to pump	60	1,500	161.0	7,211,029	1.0121	0.24
8	Oxygen rich	25	101.3	5.8	711	16.7759	7.86
9	Nitrogen rich	1	101.3	25.6	344	1.0000	0.00
10	CO ₂ rich-permeate	40	300	8.2	60,975	1.0200	0.25
11	Oil export to shore	60	2,300	161.0	7,211,029	1.0123	0.24
12	Natural gas (fuel)	38	4,800	1.5	73,798	1.0200	0.25
13	Waste water	18	4	1.4	70	0.0000	0.00
14	Captured CO ₂ to compression	366	100	5.9	2,901	1.1704	0.32
15	Waste water	23	multiple	1.8	5	0.0000	0.00
16	Captured CO ₂ to injection	101	45,000	4.2	2,901	1.1839	0.33
17	Natural gas export	113	24,500	26.5	1,286,320	1.0282	0.25
18	CO ₂ (from well) to injection	130	45,000	8.2	63,442	1.0861	0.29

19	Primary separation (Heating requirement)	150	-	-	1,985	16.1784	5.70
20	Net power (to compression systems)	-	-	-	27,477	2.3708	1.08
21	NG export compression power	-	-	-	7,822	2.3708	1.08
22	CO ₂ (well) to injection compression power	-	-	-	3,458	2.3708	1.08
23	Air separation compression power	-	-	-	5,970	2.3708	1.08
24	Oil pump power	-	-	-	447	2.3708	1.08
25	Captured CO ₂ injection compression power	-	-	-	1,732	2.3708	1.08
26	Gas compression power	-	-	-	8,039	2.3708	1.08
27	NG to compression	38	4,800	26.5	1,280,183	1.0200	0.25

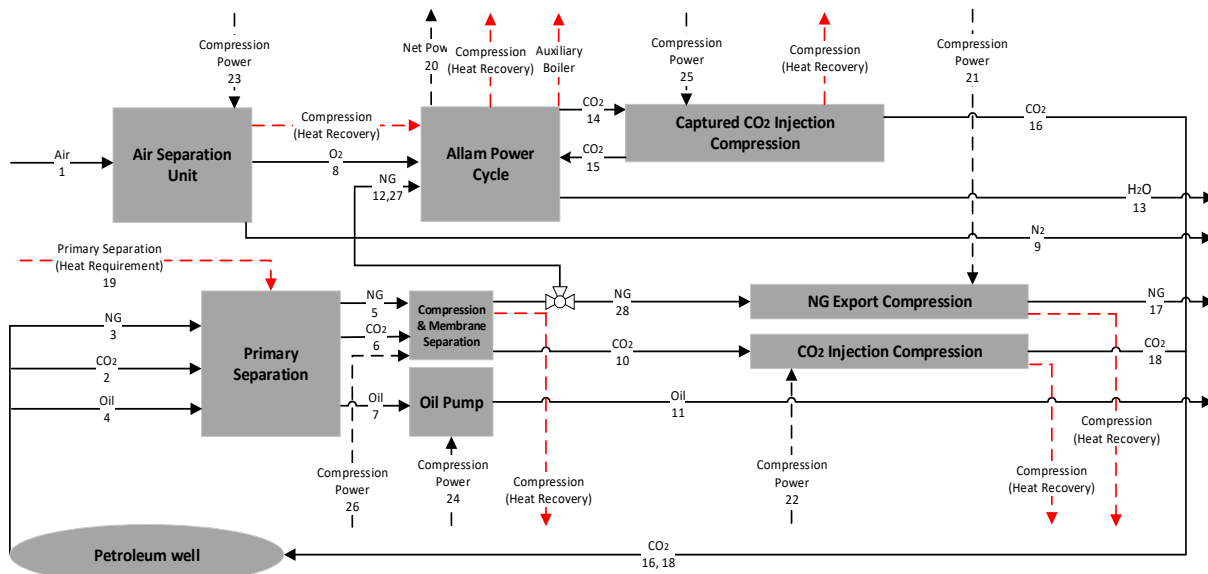


Figure A.4. Offshore platform integrated to an Allam power cycle. Calculation scheme for the unit exergy cost and specific CO₂ emissions.

Table A.4. Thermodynamic properties and exergy cost of selected streams in the Fig A.4. Offshore platform integrated to an Allam power cycle.

N ^o	Name	T (°C)	P (kPa)	m (kg/s)	B ^T (kW)	c (kJ/kJ)	cc ₀₂ (gco ₂ /MJ)
1	Combustion air	25	101.3	17.8	0	1.0000	0.00
2	CO ₂ (well)	40	1500	8.2	61,856	1.0081	0.25
3	Natural gas (well)	40	1,500	28	1,349,493	1.0081	0.25
4	Oil (well)	40	1,500	161	7,211,029	1.0081	0.25
5	NG to compression & membrane	40	1,500	28.0	1,349,493	1.0096	0.26
6	CO ₂ to compression & membrane	40	1,500	8.2	61,856	1.0096	0.26
7	Oil to pump	60	1,500	161	7,211,029	1.0096	0.26
8	Oxygen rich	25	101.3	3.3	403	13.4496	103.51
9	Nitrogen rich	1	101.3	14.5	195	1.0000	0.00
10	CO ₂ rich-permeate	40	300	8.2	60,975	1.0155	0.32
11	Oil export to shore	60	2,300	161	7,211,029	1.0098	0.26
12	Natural gas (fuel)	38	4,800	0.9	42,758	1.0155	0.32
13	Waste water	30	3,000	1.9	112	0.0000	0.00
14	Captured CO ₂ to compression	30	3,000	60.2	37,543	1.1721	1.89

15	CO ₂ recycled	40	10,000	57.9	38,311	1.2361	2.76
16	Captured CO ₂ to injection	78	45,000	2.3	1,611	1.3170	3.75
17	Natural gas export	113	24,500	27	1,312,951	1.0212	0.40
18	CO ₂ (from well) to injection	130	45,000	8.2	63,442	1.0614	0.94
19	Primary separation (Heating requirement)	150	-	-	1,985	6.8843	37.64
20	Net power (to compression systems)	-	-	-	27,237	1.9139	14.22
21	NG export compression power	-	-	-	7,984	1.9139	14.22
22	CO ₂ (well) to injection compression power	-	-	-	3,458	1.9139	14.22
23	Air separation compression power	-	-	-	3,384	1.9139	14.22
24	Oil pump power	-	-	-	447	1.9139	14.22
25	Captured CO ₂ injection compression power	-	-	-	3,919	1.9139	14.22
26	Gas compression power	-	-	-	8,039	1.9139	14.22
27	Auxiliary boiler fuel	38	4,800	0.09	4,536	1.0155	0.32
28	NG to compression	38	4,800	27	1,306,687	1.0155	0.32

Table A.5 lists the auxiliary equations considered in the allocation of the exergy cost and specific CO₂ through the utility systems and processing units of the different platform layouts.

Table A.5. Auxiliary equations considered in order to calculate unit exergy and CO₂ emissions costs of the streams on the different platforms.

Platform layout with CHP unit and CCS approach				
Control volume	Conventional	Amines-based	S-Graz cycle-powered	Allam cycle-powered
Power Cycle	$c_{20} = 0$ $c_q = \frac{c_1 B_1 + c_2 B_2}{B_1 + B_2}$	$c_9 = 0$ $c_q = \frac{c_1 B_1 + c_2 B_2}{B_1 + B_2}$ $= c_{30}$	$c_{13} = 0$ $c_{14} = \frac{c_8 B_8 + c_{12} B_{12}}{B_8 + B_{12}} = c_q$	$c_{13} = 0$ $c_{14} = \frac{c_8 B_8 + c_{12,27} B_{12,27} + c_{15} B_{15}}{B_8 + B_{12,27} + B_{15}} = c_q$
Primary Separation	$c_{10} = c_9 = c_8$	$c_{11} = c_{12}$ $= c_{13}$	$c_7 = c_5$ $c_6 = c_5$	$c_5 = c_6 = c_7$
Compression & Membrane separation	$c_{15} = c_{14}$ $c_q = c_{13}$	$c_{13} = c_{14}$ $c_q = c_{10}$	$c_{10} = c_{27}$ $c_{26} = c_q$	$c_q = c_{26}$ $c_{10} = c_{28}$
NG export compression	$c_q = c_{16}$	$c_q = c_{26}$	$c_q = c_{21}$	$c_q = c_{21}$
CO ₂ injection compression	$c_q = c_{17}$	$c_q = c_{27}$	$c_q = c_{22}$	$c_q = c_{22}$
Amines loop carbon capture	-	$c_{22} = 0$ $c_{21} = c_q$ $c_{19} = c_7$	-	-
Captured CO ₂ injection compression	-	$c_q = c_{25}$ $c_{23} = 0$	$c_{15} = 0$ $c_q = c_{25}$	$c_q = c_{25}$ $c_{15} = c_{16}$
Air separation unit	-	-	$c_9 = c_1 = 1$ $c_{23} = c_q$	$c_1 = c_9 = 1$ $c_q = c_{23}$

References

1. Figueroa, J.D., Fout, T., Plasynski, S., McIlvried H., Srivastava, R. D., *Advances in CO₂ capture technology—The U.S. Department of Energy's Carbon Sequestration Program*. International Journal of Greenhouse Gas Control, 2008(2): p. 9-20.
2. IPCC, *Climate Change 2014: Mitigation of Climate Change*, in *Working Group III Contribution to the Fifth Assessment Report of the Intergovernmental Panel on Climate Change*. 2014, International Panel on Climate Change (IPCC). p. 1454.
3. IEA, *Energy and Climate Change, World Energy Outlook Special Report*. 2015, International Energy Agency. p. 1-200.
4. Zappa, W., Junginger, M., van den Broek, M., *Is a 100% renewable European power system feasible by 2050?* Applied Energy, 2019. **233-234**: p. 1027-1050.
5. Leung, D.Y.C., Caramanna, G., Mercedes Maroto-Valer, M. , *An overview of current status of carbon dioxide capture and storage technologies*. Renewable and Sustainable Energy Reviews, 2014. **39**: p. 426-443.
6. Boait, P., Advani, V., Gammon, R., *Estimation of demand diversity and daily demand profile for off-grid electrification in developing countries*. Energy for Sustainable Development, 2015. **29**: p. 135-141.
7. Zhang, Q., Li, H., McLellan, B., *An Integrated Scenario Analysis for Future Zero-Carbon Energy System*. Energy Procedia, 2014. **61**: p. 2801-2804.
8. IEA, *Outlook for Natural Gas*, in *World Energy Outlook 2017*, International Energy Agency. p. 449-460.
9. Heitmeir, F., Sanz, W., Jericha, H., *1.3.1.1. Graz Cycle – a Zero Emission Power Plant of Highest Efficiency*, in *The Gas Turbine Handbook*, 2006, National Energy Technology Laboratory.
10. Mancuso, L., Ferrari, N., Paolo, C., Martelli, E., Romano, M., *Oxy-combustion turbine power plants. Report: 2015/05*. 2015, International Energy Agency.
11. Sanz, W., Jericha, H., Luckel, F., Göttlich, E., Heitmeir, F. *A further step towards a Graz cycle power plant for CO₂ capture*. in *ASME Turbo Expo 2005: Power for Land, Sea and Air*. 2005. Reno-Tahoe, Nevada, USA.
12. Ellsworth, B. *Petrobras to begin offshore CO₂ sequestration*. 2011.
13. Halliburton. *Supergiant Lula Brings CO₂ EOR Advances*. 2012.
14. Beck, B., Cunha, P., Ketzer, M., Machado, H., Rocha, Paulo S., Zancan, F., de Almeida, A. Pinheiro, D., *The current status of CCS development in Brazil*. Energy Procedia, 2011. **4**: p. 6148-6151.
15. Carranza-Sánchez, Y., Oliveira Jr, S., *Exergy analysis of offshore primary petroleum processing plant with CO₂ capture*. Energy, 2015. **88**: p. 46-56.
16. Carranza-Sánchez, Y.A., Oliveira Junior, S., da Silva, J.A.M., Nguyen, T.V. *Energy and exergy performance of three FPSO operational modes*. in *Proceedings of the 23rd ABCM International Congress of Mechanical Engineering*. 2015.
17. Flórez-Orrego, D., Silva, J.A.M., Velásquez, H., Oliveira Jr., S., *Renewable and non-renewable exergy costs and CO₂ emissions in the production of fuels for Brazilian transportation sector*. Energy, 2015. **88**: p. 18-36.
18. Silva, J.A.M., Flórez-Orrego, D., Oliveira Jr, S., *An exergy based approach to determine production cost and CO₂ allocation for petroleum derived fuels*. Energy, 2014. **67**: p. 490-495.
19. Silva, J.A.M., Oliveira Junior, S., *Unit exergy cost and CO₂ emissions of offshore petroleum production*. Energy, 2018. **147**: p. 757-766.
20. Nakashima, C.Y., Oliveira Jr. S., Caetano, E. F., *Subsea multiphase pumping system x gas lift: an exergo-economic comparison*. Thermal Engineering, 2004. **3**(2): p. 107-114.
21. Nguyen, T.V., Fülöp, T.G., Breuhaus, P., Elmegaard, B., *Life performance of oil and gas platforms: Site integration and thermodynamic evaluation*. Energy, 2014. **73**: p. 282-301.
22. Nguyen, T.V., Voldsund, M., Breuhaus, P., Elmegaard, B., *Energy efficiency measures for offshore oil and gas platforms*. Energy, 2016. **117**: p. 325-340.
23. Baker, R., Lokhandwala, K., *Natural Gas Processing with Membranes: An Overview*. Industrial & Engineering Chemistry Research, 2008. **47**(7): p. 2109-2121.
24. Nguyen, T.V., Voldsund, M., Elmegaard, B., Ertesvåg, I.S., Kjelstrup, S., *On the definition of exergy efficiencies for petroleum systems: Application to offshore oil and gas processing*. Energy, 2014. **73**, p.264-281.
25. IEAGHG, *CO₂ Capture as a factor in power station investment*. 2006: IEA Greenhouse Gas R&D Programme.

26. Jericha, H., *Efficient steam cycles with internal combustion of hydrogen and stoichiometric oxygen for turbines and piston engines*. International Journal Hydrogen Energy, 1985. **12**(5): p. 345-354.
27. Jericha, H., Göttlich, E. *Conceptual design for an industrial prototype gas cycle power plant*. in *ASME TURBO EXPO 2002*. Amsterdam.
28. Allam et al., *System and method for high efficiency power generation using a carbon dioxide circulating working fluid*. 2011, Palmer Labs, LLC.
29. Allam et al., *System and method for high efficiency power generation using a carbon dioxide circulating working fluid*. 2013, 8 Rivers Capital, LLC, Durham, NC (US).
30. Allam et al., *High efficiency and low cost of electricity generation from fossil fuels while eliminating atmospheric emissions, including carbon dioxide*. Energy Procedia, 2013. **37**: p. 1135-1149.
31. Allam et al., *Demonstration of the Allam Cycle: An update on the development status of a high efficiency supercritical carbon dioxide power process employing full carbon capture*. Energy Procedia, 2017. **114**: p. 5948-5966.
32. Net Power., *NET Power Achieves Major Milestone for Carbon Capture with Demonstration Plant First Fire*, in *The Company Is Now Operating Its Low-Cost, Emissions-Free Natural Gas Power System*. 2018.
33. Penkuhn, M., Tsatsaronis, G., *Exergy Analysis of the Allam Cycle*, in *The 5th International Symposium – Supercritical CO₂ Power Cycles*. 2016: San Antonio, Texas.
34. van der Ham, L.V., J. Gross, and S. Kjelstrup, *Two performance indicators for the characterization of the entropy production in a process unit*. Energy, 2011. **36**(6): p. 3727-3732.
35. Agrawal, R., Herron, D., *Air Liquefaction: Distillation*, in *Encyclopedia of Separation Science*, ed. P. I. Wilson, C., Cooke, M. 2000: Academic Press.
36. Fu, C., Gundersen, T., *Using exergy analysis to reduce power consumption in air separation units for oxy-combustion processes*. Energy, 2012. **44**: p. 60-68.
37. National Energy Technology Laboratory., *Quality guidelines for energy system studies - CO₂ Impurity Design Parameters*, US Department of Energy., Editor. 2012, Office of Program Planning and Analysis.
38. Abdollahi-Demneh, F., Moosavian, M., Omidkhah, M., Bahmanyar, H., *Calculating exergy in flowsheeting simulators: A HYSYS implementation*. Energy, 2011. **36**(8): p. 5320-5327.
39. Oliveira Júnior, S., Van Hombeeck, M., *Exergy analysis of petroleum separation processes in offshore platforms*. Energy Conversion and Management, 1997. **38**(15-17): p. 1577-1584.
40. Oliveira Jr., S., *Exergy: Production, Cost and Renewability* 2013, Sao Paulo: Springer.
41. Silva, J.A.M., Oliveira, Jr., S., Pulgarin, J., Velasquez, H., Molina, A., *On the exergy determination for petroleum fractions and separation processes efficiency*. Heat Transf. Eng, 2015. **36**(11): p. 974-983.
42. Silva, J.A.M., *Exergoenvironmental Performance of Petroleum Processing [In Portuguese]*. 2017: Novas Edicoes Academicas.
43. Flórez-Orrego, D., Silva, J. A. M., Oliveira Jr, S., *Exergy and environmental comparison of the end use of vehicle fuels: The Brazilian case*. Energy Conversion and Management, 2015. **100**: p. 220-231.
44. Flórez-Orrego, D., *Thermodynamic and environmental comparison of the production and end-use routes of vehicle fuels derived from petroleum and natural gas, biofuels, hydrogen and electricity [In Portuguese]*, in *Department of Mechanical Engineering*. 2014, University of São Paulo: São Paulo. p. 229.
45. Flórez-Orrego, D., Oliveira Junior, S. *On the efficiency, exergy costs and CO₂ emission cost allocation for an integrated syngas and ammonia production plant*. Energy, v. **117**, Part 2, p. 341-360, 2016.
46. Flórez-Orrego, D., Sharma, S., Oliveira Junior, S., Maréchal, F. *Combined exergy analysis, energy integration and optimization of syngas and ammonia production plants: A cogeneration and syngas purification perspective*. Journal of Cleaner Production, v. **244**, p. 118647.
47. Beysel, G. *Enhanced Cryogenic Air Separation: A proven Process applied to Oxyfuel*. The Linde Group. in *1st Oxyfuel Combustion Conference*. 2009. Cottbus.
48. Flórez-Orrego, D., Nascimento Silva, F., Oliveira Junior, S. *Syngas production with thermo-chemically recuperated gas expansion systems: An exergy analysis and energy integration study*. Energy, v. **178**, p. 293-308.
49. Suphanit, B., *Design of internally heat-integrated distillation column (HIDiC): Uniform heat transfer area versus uniform heat distribution*. Energy, 2010. **35**(3): p. 1505-1514.
50. Dunbar, W.R., Lior, N., *Sources of combustion irreversibility*. Combustion Science and Technology, 1994. **103**(1-6): p. 41-61.
51. Tuong-Van Nguyen; Tamás Gábor Fülöp; Peter Breuhaus; Brian Elmegaard, *Life performance of oil and gas platforms: Site integration and thermodynamic evaluation*. Energy, 2014. **73**: p. 282-301.
52. Freire, R.L.A., Oliveira Junior, S., *Lifetime exergy analysis of electricity and hot water production systems in offshore projects with multiple platforms*. in *ENCIT*. 2018. Águas de Lindóia, SP, Brazil.

53. Biello, D., *Can Carbon Capture Technology Be Part of the Climate Solution?*, in *Yale Environment* 360. 2014, Yale School of Forestry & Environmental Studies.
54. Broecks et al., *Persuasiveness, importance and novelty of arguments about Carbon Capture and Storage*. *Environmental Science & Policy*, 2016. **59**: p. 58-66.
55. NOAH Friends of the Earth Denmark., *10 arguments against CCS*: NOAH Friends of the Earth Denmark.
56. McGlade, C., Ekins, P., *The geographical distribution of fossil fuels unused when limiting global warming to 2 °C*. *Nature*, 2015. **517**: p. 187–190.